Intrinsic rotation and electric field shear

Ö. D. Gürcan[a] and P. H. Diamond
Center for Astrophysics and Space Sciences, University of California, San Diego, La Jolla, California 92093-0424

T. S. Hahm
Princeton Plasma Physics Laboratory, Princeton, New Jersey 08543-0451

R. Singh
Institute for Plasma Research, Bhat, Gandhinagar-382 428, India

(Received 23 October 2006; accepted 28 February 2007; published online 26 April 2007)

A novel mechanism for the generation and amplification of intrinsic rotation at the low-mode to high-mode transition is presented. The mechanism is one where the net parallel flow is accelerated by turbulence. A preferential direction of acceleration results from the breaking of $k_\parallel \rightarrow -k_\parallel$ symmetry by sheared $\mathbf{E}\times\mathbf{B}$ flow. It is shown that the equilibrium pressure gradient contributes a piece of the parallel Reynolds stress, which is nonzero for vanishing parallel flow, and so can accelerate the plasma, driving net intrinsic rotation. Rotation drive, transport, and fluctuation dynamics are treated self-consistently. © *2007 American Institute of Physics*.
[DOI: 10.1063/1.2717891]

I. INTRODUCTION

Neutral beam injection (NBI) has long been the heating method of choice for tokamak plasmas and, as a consequence, the tokamak confinement database is dominated by entries from NBI-heated discharges. Given that, and the fact that unbalanced NBI naturally produces toroidal rotation, toroidal angular momentum transport has also been the subject of intensive study for some time now. Pioneering experimental investigations established that the toroidal viscosity χ_ϕ was turbulent and roughly comparable to the ion thermal diffusivity[1] (i.e., $\chi_\phi \sim \chi_i$) in accordance with expectations based upon ion temperature gradient driven (ITG) or drift wave turbulence models.[2] Also, toroidal viscosity was observed to be quenched, along with χ_i and the particle diffusivity D_n in ion internal transport barrier (ITB) regimes. Taken together, these observations constituted a plausible phenomenology that the momentum transport was diffusive, driven by small-scale drift-ITG turbulence, and roughly comparable to the ion heat transport.

This blissful state of consciousness was disturbed by the observation that an "off-diagonal" contribution to the momentum transport, which is proportional to ∇P (Ref. 3), was necessary to fit the experimentally observed profile evolution in the JFT-2M (Ref. 4) tokamak, suggesting that the Reynolds stress driven flux should have the form $\langle \tilde{v}_r \tilde{v}_\phi \rangle = -\chi_\phi \partial_r \langle v_\phi \rangle + V \langle v_\phi \rangle$, where $V \sim V\ (\nabla P)$. Note that for $\chi_\phi \sim \chi_i$, $V<0$ was needed in order to explain the reported inward "pinch" of momentum. The "bliss" of ignorance was then *destroyed* by the discovery of "spontaneous" or "intrinsic" rotation when toroidal rotation of the central plasma in Alcator-C-Mod (Ref. 5) for both the Ohmically heated case and the ion cyclotron resonance frequency (ICRF) driven case (i.e., no external momentum input in either case) was observed.[6,7] Recently, this observation has been verified in other tokamaks.[9,10] More recently, in the TCV tokamak,[11] a critical density for bifurcation and onset of toroidal rotation was observed in the low (*L*)-mode regime.[12] Also, study of the toroidal momentum transport in JT-60U (Ref. 13) with perpendicular NBI heating suggests that fast particle losses due to edge magnetic ripple may play an important role in driving toroidal rotation.[14] Related perturbative experiments using parallel NBI drive suggest that along with the usual momentum diffusivity, an inward flux of toroidal flow is needed to explain observed rotation profiles. It is also important to note that the Reynolds stress becomes significant during the toroidal momentum transport activity,[15,16] suggesting that the observed momentum transport is linked to fluctuations. Thus, it seems eminently fair to say that the early, superficially simple story about toroidal momentum transport has vanished and has been replaced by a rich but complex phenomenology, the most prominent element of which is spontaneous rotation.

Here, by spontaneous or intrinsic rotation, we mean rotation which occurs in the absence of identifiable NBI or wave external torques and which unambiguously exceeds the predictions of neoclassical theory. Note that intrinsic rotation has manifested itself both as rotation in the absence of any NBI input *and* as a finite offset in the plot of rotation velocity versus torque.[10] While intrinsic rotation has been observed in all tokamak parameter regimes and for all heating methods, *the phenomenology of intrinsic rotation is demonstrably the cleanest and most consistent for high (H)-mode discharges*. For those plasmas, the intrinsic rotation is observed to be in the cocurrent direction and to scale with the diamagnetic β (i.e., $v/v_A \lesssim \beta_N$), which means that toroidal rotation decreases as the poloidal current increases (with pressure also increasing) for the cocurrent rotation case.[17] Initially regarded as something of a curiosity, spontaneous rotation is now a critical focus of research, since plasma rotation is

[a]URL: http://diamnd.ucsd.edu, Electronic mail: ogurcan@ucsd.edu

essential to avoid disruption by resistive wall modes (RWM), and because NBI is thought not to be a practical means to drive rotation in the International Thermonuclear Experimental Reactor (ITER) (Ref. 18).

The surge of interest in spontaneous rotation has sparked renewed interest in the subject of toroidal momentum transport. In particular, a likely element in a dynamical model of spontaneous rotation is a nondiffusive inward flux of toroidal momentum, which could enhance momentum confinement and lead to a peaked rotation profile or produce a spin up by an inward flow of momentum from edge sources, which are, as yet, not understood. Indeed there is some discussion of the edge as a possible momentum source in the current research literature.[6–8] Of course, the total flux of parallel momentum $\Pi_\parallel$ consists of both convective and Reynolds stress driven pieces, i.e.,

$$\Pi_\parallel \approx \langle v_\parallel \rangle \langle \tilde{v}_r \tilde{n} \rangle + \langle n \rangle \langle \tilde{v}_r \tilde{v}_\parallel \rangle,$$

where the particle flux usually contains an inward flow or "pinch," as well as diffusion, i.e.,

$$\Gamma_n \equiv \langle \tilde{v}_r \tilde{n} \rangle \approx -D \frac{\partial \langle n \rangle}{\partial r} + V \langle n \rangle$$

with $V<0$. Hence, one possible channel for inward, nondiffusive momentum transport is simply the familiar convective particle pinch. While the existence of a particle pinch is well established in the tokamak phenomenology, the *dynamics* of the particle pinch remain a topic of active study. Possible candidate mechanisms for the particle pinch are the thermoelectric coupling and turbulent equipartition.

Apart from the convective pinch, the other possible channel for nondiffusive transport of momentum is via the Reynolds stress $\langle \tilde{v}_r \tilde{v}_\parallel \rangle$. As we will show later in the paper, *breaking of* $k_\parallel \rightarrow -k_\parallel$ *symmetry is required for* $\langle \tilde{v}_r \tilde{v}_\parallel \rangle$ *to have a nondiffusive component*. Interestingly radially sheared $\mathbf{E}\times\mathbf{B}$ velocity is one such $k_\parallel \rightarrow -k_\parallel$ symmetry-breaking mechanism in that $\langle v_E \rangle' \neq 0$ shifts the centroid of the fluctuation spectrum structure function to a nonzero value, so that the spectrally averaged $k_\parallel$, written as $\langle k_\parallel \rangle$, becomes nonzero and proportional to $\langle v_E \rangle'$. Furthermore, while $\mathbf{E}\times\mathbf{B}$ flow shear is not the unique mechanism for breaking of $k_\parallel \rightarrow -k_\parallel$ symmetry, it appears to be the most robust and directly links the nondiffusive Reynolds stress to the dynamics of transport bifurcations, in general, and to the low-mode to high-mode (*L-H*) transition in particular. The latter observation is indeed relevant, since the phenomenology of intrinsic rotation is clearest in the *H* mode. Of course, electric field shear also tends to reduce or quench fluctuations and transport, and so will, ultimately, act to turn off all elements of the Reynolds stress $\langle \tilde{v}_r \tilde{v}_\parallel \rangle$. Thus a self-consistent treatment is crucial in order to properly evaluate the tradeoff between increased symmetry breaking and decreased fluctuation intensity.

Historically, the role of E_r' as an important element in the off-diagonal momentum flux was identified previously.[19,20] Also, a basic picture of off-diagonal momentum flux based on an imbalance between populations of waves propagating in the parallel direction was suggested.[21,22] In fact, neoclassical theory has long been aware of the importance of angular momentum transport.[23] Also, an "Onsager symmetric" particle/momentum pinch effect was mentioned in neoclassical literature.[24] Another significant modeling attempt along these lines was a rather detailed study of neoclassical momentum transport,[25] clearly suggesting a mode-dependent "pinch" term. In this study, which employs a model based on electrostatic fluctuation ripple, the momentum pinch term is a mixture of both the Reynolds stress "flow pinch" (which is a curvature effect for this case) and the convective pinch (driven convectively by the particle transport). Recent quasilinear modeling, which does not include the E_r' effect, found that no substantial pinch term exists for parallel flow.[26] Similar phenomena have been observed in stellarators,[15] tokamaks,[6,16] and reversed field pinches.[27]

In this paper we calculate the diffusive and nondiffusive flux of parallel momentum driven by ITG turbulence in a cylindrical plasma model, with a self-consistent, sheared mean electric field. Both the convective $\langle \tilde{v}_r \tilde{n} \rangle \langle v_\parallel \rangle$ and parallel Reynolds stress contributions $\langle n \rangle \langle \tilde{v}_r \tilde{v}_\parallel \rangle$ are discussed, but we focus primarily upon the latter. In the spirit of mean-field electrodynamics we show that the parallel Reynolds stress can be expressed in the form

$$\langle \tilde{v}_r \tilde{v}_\parallel \rangle \approx S(x) + V(x) \langle v_\parallel \rangle - D(x) \frac{\partial \langle v_\parallel \rangle}{\partial x},$$

where $S(x)$ is *independent* of parallel flow, $V(x)$ is the convective flow velocity, and $D(x)$ is the usual turbulent diffusion, which corresponds to χ_ϕ. In this model $S(x)$ and $V(x)$ result *exclusively* from broken $k_\parallel \rightarrow -k_\parallel$ symmetry, which is induced by radial electric field shear. We show that the velocity-independent stress $S(x)$ is driven by the pressure gradient contribution to the electric field shear $[\sim(\nabla P/n)']$ and that $V(x)$ is driven by the toroidal velocity contribution $[\sim(B_\theta \langle v_\phi \rangle)']$. Note that $S(x)$ is a novel effect and has no analog in diffusion-convection models of particle transport. $S(x)$ drives a flux of $\langle v_\parallel \rangle$ in the absence of initial $\langle v_\parallel \rangle$, and $-\partial(\langle n \rangle S)/\partial x$ constitutes a *local momentum source*. Of course, wave momentum is required for such a local source, and this is provided by the symmetry breaking, which renders $\langle k_\parallel \rangle \neq 0$ so the wave momentum $P_w \sim \Sigma_k k_\parallel N$ is also nonzero. Here N is the wave quanta or action density. Since it is finite for $\langle v_\parallel \rangle = 0$, $S(x)$ may be said to exert a net force on the plasma so that (in the absence of flow) the velocity increment $\Delta v_\parallel = v_\parallel(0) - v_\parallel(a)$ grows according to

$$\frac{\partial \Delta v_\parallel}{\partial t} = S(a) - S(0) \approx S(a),$$

where a is the plasma "boundary" between the core and edge, or scrape off layer (SOL) regions. We note that $S(0) \approx 0$, since $\nabla P \sim \nabla n \sim 0$ near the left boundary. With turbulent viscous diffusion ν_T of a finite flow, the steady-state velocity gradient increment is then

$$\Delta\left(\frac{\partial \langle v_\parallel \rangle}{\partial x}\right) = -\frac{S(a)}{\nu_T}.$$

Thus we see that the stress $S(x)$, along with the edge conditions which set $\langle v_\parallel(a) \rangle$ and $\partial \langle v_\parallel \rangle / \partial x|_a$, determine the structure of the intrinsic rotation profile. For ITG turbulence,

$S(x)<0$ (inward flux) and $V(x)<0$ (small but outward flow). At first glance, $S(x)$ increases with ∇P, suggesting stronger intrinsic rotation in the H mode, in accordance with observations. However a self-consistent treatment of the fluctuation intensity along with the momentum flux is required, since fluctuation levels drop as $\langle v_E\rangle'$ increases. Results of such a self-consistent study indicate that the rotation generation mechanism is robust since, although$S$ and ν_T decrease with increasing $\langle v_E\rangle'$, the ratio S/ν_T *increases* with $\langle v_E\rangle'$, so that the core rotation increases. We study the sensitivity of the resulting intrinsic rotation to the (edge) boundary conditions on $\langle v_\parallel(x)\rangle$ using a simplified transport model.

The remainder of this paper is organized as follows. Section II introduces the basic formulation of toroidal momentum transport for a simple fluid ITG model using quasilinear theory. In Sec. II A, the edge boundary conditions and how they lead to a bulk rotation of the plasma are discussed, while in Sec. II B the basic self-consistent transport model is given. Section III is devoted to numerical results and discussions of the implications of this model. In Sec. IV we give a fully gyrokinetic derivation, in cylindrical geometry, of the relevant stresses that appear in the model. Here, Sec. IV A introduces the two-scale kinetic framework. The moments of the drift kinetic equation, which describe the slow evolution, are computed in Sec. IV B, and fluctuating moments of the gyrokinetic distribution function and the stresses resulting from these fluctuations are computed in Sec. IV C. The eigenmode equation resulting from the gyrokinetic formulation is derived in Sec. IV D and its fluid limit is given in Sec. IV E. In Sec. IV F, we solve this eigenmode equation and compute the shifts caused by $\mathbf{E}\times\mathbf{B}$ shear for the ITG and electron drift wave branches. After a brief discussion of momentum versus flow, in Sec. V, we conclude in Sec. VI. The higher-order corrections to the Reynolds stresses, which are calculated in the text within the fluid approximation, are given in the Appendix.

II. FORMULATION

The equation for mean parallel velocity in a simple fluid plasma model can be written as

$$\frac{\partial}{\partial t}\bar{v}_\parallel(x)+\frac{\partial}{\partial x}\langle\tilde{v}_{\mathrm{Ex}}\tilde{v}_\parallel\rangle=\nu\frac{\partial^2}{\partial x^2}\bar{v}_\parallel, \tag{1}$$

where $\bar{v}_\parallel$ is the mean parallel flow velocity, $\tilde{v}_\parallel$ is the fluctuating parallel flow velocity, $\tilde{v}_{\mathrm{Ex}}$ is the radial component of the fluctuating $\mathbf{E}\times\mathbf{B}$ velocity, and ν is the collisional parallel viscosity. Note that we use $\langle\cdot\rangle$, and $\overline{(\cdot)}$ interchangeably throughout the text. These can be interpreted as averages over the time scales related to the fluctuations. The parallel Reynolds stress $\langle\tilde{v}_{\mathrm{Ex}}\tilde{v}_\parallel\rangle$, which controls momentum transport, can, in general, be written as

$$\langle\tilde{v}_{\mathrm{Ex}}\tilde{v}_\parallel\rangle\approx-\nu_T\frac{\partial\bar{v}_\parallel}{\partial x}+U_r^{(\phi)}\bar{v}_\parallel+S, \tag{2}$$

where ν_T is a turbulent viscosity coefficient, $U_r\bar{v}_\parallel$ is a convective flow term, where the direction of the flow depends on the sign of U_r, and $S\equiv S_{x\parallel}$ is the "zero-flow" component of the off-diagonal stress density, which has no direct dependence on $\bar{v}_\parallel$ or $\partial\bar{v}_\parallel/\partial x$. Note that S appears in addition to the usual "D and V model," and may have a significant role, especially in the generation of toroidal flow. In the spirit of mean-field electrodynamics, one can formulate $\langle\tilde{v}_{\mathrm{Ex}}\tilde{v}_\parallel\rangle\equiv R(\bar{v}_\parallel,\partial\bar{v}_\parallel/\partial x)$, as a Taylor series expansion of R for small arguments,

$$\langle\tilde{v}_{\mathrm{Ex}}\tilde{v}_\parallel\rangle\approx R(0,0)+\frac{\partial R(0,\nabla_r\bar{v}_\parallel)}{\partial(\nabla_r\bar{v}_\parallel)}\nabla_r\bar{v}_\parallel+\frac{\partial R(\bar{v}_\parallel,0)}{\partial\bar{v}_\parallel}\bar{v}_\parallel,$$

where

$$S\equiv R(0,0),\quad \nu_T\equiv-\frac{\partial R(0,\nabla_r\bar{v}_\parallel)}{\partial(\nabla_r\bar{v}_\parallel)}\quad\text{and}\quad U_r^{(\phi)}\equiv\frac{\partial R(\bar{v}_\parallel,0)}{\partial\bar{v}_\parallel}.$$

Note that writing (2) as a diffusion and a radial flow would be misleading, and it is clear that we need something *independent of* the parallel shear flow itself in order to obtain a nonzero S. This zero mean flow component of the parallel Reynolds stress quite likely determines the "offset" in the plot of injected momentum versus toroidal flow.

In order to compute the stress terms, one can follow a quasilinear closure using a simple linear response based upon ITG turbulence, for which the basic equations are

$$D_t\tilde{v}_\parallel-v_{ti}v_\parallel'(x)\left(\rho_i\frac{\partial}{\partial y}\right)\left(\frac{e\tilde{\Phi}}{T_i}\right)=-v_{ti}^2\nabla_\parallel\left(\frac{e\tilde{\Phi}}{T_i}+\frac{\tilde{P}}{P_i}\right), \tag{3}$$

$$D_t\tilde{P}-v_{ti}\bar{P}'(x)(\rho_i\partial_y)\left(\frac{e\tilde{\Phi}}{T_i}\right)=0. \tag{4}$$

The parallel stress can then be easily computed from these equations, and is

$$\langle\tilde{v}_{\mathrm{Ex}}\tilde{v}_\parallel\rangle=-\mathrm{Re}\sum_k iv_{ti}^2\rho_ik_y\left[\frac{v_{ti}k_y}{\omega_k}\frac{\rho_i}{v_{ti}}\frac{\partial}{\partial x}\bar{v}_\parallel+\frac{v_{ti}k_y}{\omega_k}\frac{v_{ti}k_\parallel}{\omega_k}\frac{\rho_i}{\bar{P}}\frac{\partial}{\partial x}\bar{P}-\frac{v_{ti}k_\parallel}{\omega_k}\right]\left|\frac{e\Phi_k}{T_i}\right|^2. \tag{5}$$

Here, the first term is the usual diffusion term and does not vanish as long as $\mathrm{Im}[\omega_k]\neq0$ (note that $\omega_k=\omega_k^{(r)}+i\gamma_k$, where γ_k is selected in accordance with causality). The second and third terms are nonlinear off-diagonal terms which can be either positive or negative depending on the sign of $\langle k_\parallel k_y\rangle$. If we use $k_\parallel=k_yx/L_s$, where x is the distance from the rational surface, the average is

$$\langle k_\parallel k_y\rangle=k_y^2\frac{\langle x\rangle}{L_s}\to0$$

for any spectrum *symmetric* with respect to the rational surface. When the sums in Eqs. (5) are computed, *both* signs of $k_\parallel$ contribute equal and opposite amounts to the sum. Since for most drift instabilities, both signs of $k_\parallel$ are equally unstable, the last two terms in the sum vanish. However, if there is breaking of $k_\parallel\to-k_\parallel$ symmetry (i.e., a dynamical preference for one sign of $k_\parallel$), a finite $\langle k_\parallel k_y\rangle$ results. Recall that a *generic effect* of $\mathbf{E}\times\mathbf{B}$ flow shear is to shift modes off the $x=0$ resonant surface (e.g., Ref. 28), thus rendering $\langle x\rangle\neq0$. In this case, the second and third terms in Eqs. (5)

FIG. 1. Acoustic waves traveling in both directions around the torus. Sheared flow changes the population density of waves in one direction relative to the other, breaking the $k_{\|} \rightarrow -k_{\|}$ symmetry and creating an imbalance between the two counterpropagating wave populations.

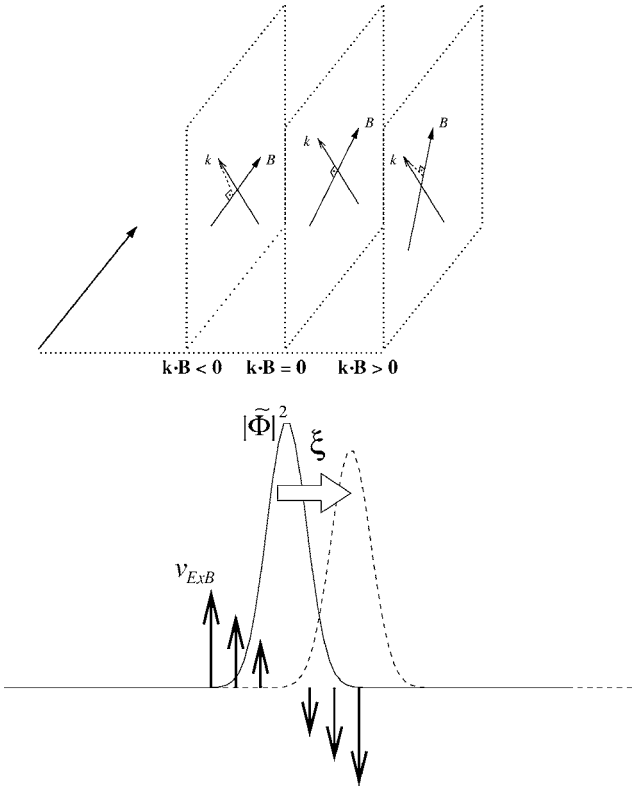

FIG. 2. Shift of the intensity fluctuation profile due to $\mathbf{E}\times\mathbf{B}$ shear.

become nonzero, thus producing a finite stress S, which is independent of mean toroidal flow. Physically, the asymmetric shift of the mode centroid off the resonant surface creates an effective imbalance in the population of sound waves traveling in the clockwise or counterclockwise directions around the torus (see Fig. 1). This imbalance creates a local torque density, thus driving spin-up and momentum transport.

Note that, the imbalance of population of sound wave densities is also an indication of the appearance of a net "wave momentum" in the fluctuations. This follows from the fact that since the wave momentum density is $\mathbf{P}=\mathbf{k}N(\mathbf{x},\mathbf{k},t)$, where $N(\mathbf{x},\mathbf{k},t)$ is the wave population density (i.e., wave action), net parallel momentum requires a net $k_{\|}$ or equivalently an imbalance in populations of copropagating and counterpropagating acoustic waves. In other words, the torque density term is finite only when the fluctuations themselves have a net parallel wave momentum. Note that this is suggestive of a complementary nondiffusive transport of wave momentum, possibly in the direction opposite to that of ions. Another obvious advantage of the net wave momentum picture is that it can be extended in a straightforward way to toroidal geometry, so that for eigenmodes having no net parallel wave momentum, the off-diagonal torque density term must necessarily vanish.

Given that $\mathbf{E}\times\mathbf{B}$ shear induces asymmetry, the expectation value of the distance from the resonant surface is equal to the centroid displacement, proportional to the $\mathbf{E}\times\mathbf{B}$ shear and given by

$$\frac{\langle x \rangle}{L_s} \equiv \frac{\xi}{L_s} \equiv -\alpha \frac{\rho_s}{L_s}\frac{L_n}{c_s}\frac{d\bar{v}_{Ey}}{dx}. \tag{6}$$

Here $\xi=\langle x \rangle$ is the centroid shift and α is a coefficient, which will be defined and calculated later. We argue that the shift of the eigenmode is due primarily to the $\mathbf{E}\times\mathbf{B}$ shear in most cases (see Figs. 2 and 3). For example, radial shear of parallel flow itself may also cause a shift, but that effect is weaker by a factor of L_n/L_s. It is precisely for this reason, and because $\mathbf{E}\times\mathbf{B}$ shear is related to transport bifurcations, that we focus on $\mathbf{E}\times\mathbf{B}$ shear as the symmetry-breaking mechanism.

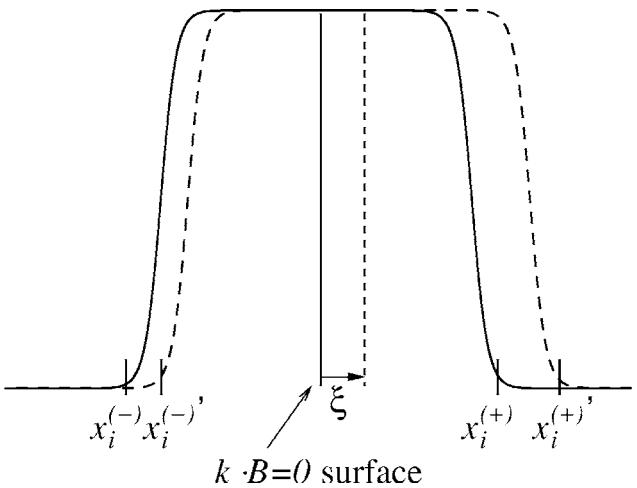

FIG. 3. Shifts in the Landau resonance points that are in the same direction resulting in a shift in the center of the fluctuation spectrum, which results in a net imbalance in wave momentum deposition.

Also, the direct wave momentum generation by the parallel flow shear leads to a modification of the diffusion term, rather than generating an off-diagonal component. Note, however, that toroidal flow shear also creates $\mathbf{E}\times\mathbf{B}$ shear (via radial force balance relation) and hence will affect the eigenmodes indirectly. This effect is included in our calculations via the radial force balance equation. The Reynolds stress, with the shift given by (6), becomes [recall $\omega_k=\omega_k^{(r)}+i\gamma_k$],

$$\langle \tilde{v}_{\mathrm{Ex}}\tilde{v}_{\parallel}\rangle = -\,\mathrm{Re}\sum_k iv_{ti}^2\left(\frac{\Omega_i}{\omega_k}\right)\rho_i^2k_y^2\Bigg[\overbrace{\frac{\rho_i}{v_{ti}}\frac{\partial}{\partial x}\bar{v}_{\parallel}}^{\text{diagonal diffusive flux}} - \underbrace{\alpha\left(\frac{v_{ti}k_y}{\omega_k}\frac{\rho_i}{\bar{P}}\frac{\partial}{\partial x}\bar{P}-1\right)\frac{\rho_s}{L_s}\frac{L_n}{c_s}\frac{d\bar{v}_{Ey}}{dx}}_{\text{nondiffusive off-diagonal flux}}\Bigg]\left|\frac{e\Phi_k}{T_i}\right|^2, \tag{7}$$

where $\mathbf{E}\times B$ flow is determined by the radial force balance relation,

$$\frac{\partial}{\partial x}\bar{v}_{Ey} = -\left(\rho_i\frac{v_{ti}}{\bar{P}}\frac{\partial^2\bar{P}}{\partial x^2} - \rho_i\frac{v_{ti}}{\bar{P}\bar{n}}\frac{\partial\bar{P}}{\partial x}\frac{\partial\bar{n}}{\partial x}\right) - \frac{1}{B_\phi}\frac{\partial}{\partial x}(\bar{v}_\phi B_\theta). \tag{8}$$

Note that if there is significant poloidal mass flow, that should also be added to the right-hand side of (8). However, poloidal flow is usually expected to be limited by the neoclassical value, which is small.

Before proceeding further, it is helpful to give the fully kinetic expression for the Reynolds stress (the derivation of which is left to later sections) in order to justify the statements that appear to be based on the simpler fluid expression. The kinetic expression for the parallel Reynolds stress is

$$\langle \tilde{v}_{Ex}\tilde{v}_{\parallel}\rangle = -\,\mathrm{Re}\sum_k i\sqrt{2}v_{ti}L_n\frac{\omega_{*e}^2}{\omega}\Gamma_0\zeta \times\Bigg[\left(\Omega\tau+1-\eta\left[\frac{1}{2}-b\frac{(\Gamma_0-\Gamma_1)}{\Gamma_0}-\zeta^2\right] - \sqrt{2}\frac{\zeta L_n}{v_{ti}}\frac{d\bar{v}_{\parallel}}{dx}\right)[1+\zeta Z(\zeta)]+\frac{\eta}{2}\Bigg]\left|\frac{e\tilde{\Phi}}{T}\right|^2. \tag{9}$$

Here $L_n=-d\ln n/dx$, $\omega_{*i}=-\Omega_i\rho_i^2L_n^{-1}k_y$, $\bar{\omega}=\omega-k_y\bar{v}_{Ey}(x)$, $\eta_i=d\ln T/d\ln n$, $\zeta=\bar{\omega}/\sqrt{2}k_{\parallel}v_{ti}$, $b=k_\perp^2\rho_i^2$, $Z(\zeta)$ is the plasma dispersion function and $\Gamma_n=I_n(b)e^{-b}$, where $I_n(b)$ is the modified Bessel function. *Note that for symmetric spectra, only those terms that are even in* ζ, *(or independent of* ζ*) will survive when the sum over* $k_{\parallel}$ *is performed*. Since $[1+\zeta Z(\zeta)]$ is even in ζ, the only term that survives the summation over the toroidal mode numbers is the term proportional to $d\bar{v}_{\parallel}/dx$. This suggests that unless $x\rightarrow -x$ *spectral symmetry is broken, the Reynolds stress term* [given in (9)] *must have the usual diffusive form of a Fick's law.* This is perhaps to be expected, but is remarkable nevertheless, since the result is based on the full kinetic theory.

Another important point is that (9) does not contain any terms explicitly proportional to $\bar{v}_{\parallel}$. Thus, the dominant contribution to "momentum convection" (i.e., part of the flux that is explicitly proportional to $\bar{v}_{\parallel}$) comes primarily from the *convective particle flux*. However, the E_r' symmetry-breaking mechanism actually introduces a term proportional to $\bar{v}_\phi$, via the radial force balance relation.

A. Global conservation relation

Note that the nondiffusive, off-diagonal terms in Reynolds stress are very important because they can act as *local* "sources" of toroidal momentum. In order to clarify this, let us consider the case when there is no explicit source of toroidal flow, such as results in the absence of direct momentum input by neutral beam injection. In that case, the conservative form of (1) says we can integrate over the radial direction to obtain

$$\frac{\partial}{\partial t}\int_0^{a_-}\bar{v}_{\parallel}(x)+\int_0^{a_-}\frac{\partial}{\partial x}\langle\tilde{v}_{Ex}\tilde{v}_{\parallel}\rangle=\int_0^{a_-}\nu\frac{\partial^2}{\partial x^2}\bar{v}_{\parallel}.$$

Neglecting the feeble collisional viscosity yields

$$\frac{\partial}{\partial t}\bar{V}_{\parallel}+\Gamma_{\parallel}(a_-)=0,$$

where $\bar{V}_{\parallel}$ is the total parallel flow and $\Gamma_{\parallel}(a_-)$ is the Reynolds stress flux at a point a_- at the edge, but within the plasma. It is important to note that if the flux only has diffusive and drift components (i.e., proportional to $\partial\bar{v}_{\parallel}/\partial x$ and $\bar{v}_{\parallel}$), and if there is no local flow or flow gradient (or external momentum source) at the edge (i.e., $\partial\bar{v}_{\parallel}/\partial x=\bar{v}_{\parallel}=0$ at a_-), then the net flow cannot change. However, an *off-diagonal term* such as the one in (7), which includes a torque density, *does not vanish at the edge even when the local flow or flow gradient vanishes*. In fact, with such an off-diagonal term, a strong edge gradient in density or temperature can drive a flux of momentum at the edge. In other words, $S(x)$ becomes a *local* source of total momentum, which exerts a net torque on the whole plasma *internal* to the point a_-,

$$\frac{\partial}{\partial t}\bar{V}_{\parallel}=\mathrm{Re}\sum_k i\alpha v_{ti}^2\left(\frac{\Omega_i}{\omega_k}\right)\rho_i^2k_y^2 \times\left(\frac{v_{ti}k_y}{\omega_k}\frac{\rho_i}{\bar{P}}\frac{\partial}{\partial x}\bar{P}(a)-1\right)\frac{\rho_s}{L_s}\frac{L_n}{c_s}\frac{d\bar{v}_{Ey}(a)}{dx}.$$

Here again, $\omega_k=\omega_k^{(r)}+i\gamma_k$. The dynamics in the SOL is outside the scope of this study and will not be addressed here. Instead, we will take either a fixed or a rotating "edge" as the boundary condition to our model. Indeed, note that even for the boundary condition $\bar{v}_{\parallel}(a_-)=0$, balance of stress and turbulent viscosity defines an edge flow gradient (i.e., $\partial\bar{v}_{\parallel}/\partial x\approx -S/\nu_T$). Since roughly $S/\nu_T\propto v_E'\propto(\partial P/\partial x)(\partial n/\partial x)$, ∇P steepening associated with the *L-H* transition can also spin up the plasma since the edge flow gradient will be proportional to ∇P. Note that since the off-diagonal torque density term draws momentum flux from the pressure and density gradients, the sources and boundary conditions for density and pressure are also important for rotation. In particular, $v_{\parallel}(a)$ along with $\partial\bar{v}_{\parallel}/\partial x\approx -S/\nu_T$, set the level of rotation.

TABLE I. Direction of various terms in Reynolds stress for different parameter regimes. Here, those cases marked with an (*) are the cases where the velocity is negative. Thus, for these cases, "outward," for instance, means an "outward flux of negative momentum" (or an inward flux of positive momentum). The convention is such that the diffusive term is always "outward." The last column denotes the effect of the $-\beta\bar{v}_\phi$ term in the radial force balance. Here, "oppose" means that term reduces the magnitude of the shear and hence opposes the tendencies given in the previous two columns, while "promote" means the flow term enhances those tendencies. Note that here "R" means $q'<0$; "Co" and "Ctr" mean the momentum drive is parallel and antiparallel to the direction of rotation, respectively, and the cases where the direction of the drive is not specified has $F_\parallel=0$.

Case	$-(\nu_{\text{neo}}+\nu_1\varepsilon)\frac{\partial}{\partial x}\bar{v}_\parallel$,	$-\alpha\varepsilon\frac{\partial}{\partial x}\bar{v}_{Ey}$,	$\alpha\varepsilon\sigma\frac{\partial}{\partial x}\bar{P}\frac{\partial}{\partial x}\bar{v}_{Ey}$,	$-\beta\bar{v}_\phi$
ITG, $\bar{v}'_{Ey}>0$	Out	Out	In	Oppose
DW, $\bar{v}'_{Ey}>0$	Out (*)	Out (*)	Out (*)	Promote
Co, ITG, $\bar{v}'_{Ey}>0$	Out	Out	In	Oppose
Ctr, ITG, $\bar{v}'_{Ey}>0$	Out (*)	Out (*)	In (*)	Promote
ITG, $\bar{v}'_{Ey}<0$	Out (*)	In (*)	Out (*)	Promote
ITG, R, $\bar{v}'_{Ey}>0$	Out	Out	In	Promote
Ctr, ITG, R, $\bar{v}'_{Ey}>0$	Out (*)	Out (*)	In (*)	Oppose

B. The model

There is one further issue related to taking the $\mathbf{E}\times\mathbf{B}$ sheared flow as the origin of symmetry breaking. Since the toroidal momentum transport is proportional to the spectral form factor shift, and the shift is proportional to the $\mathbf{E}\times\mathbf{B}$ shear, one may naively expect an increase in transport when $\mathbf{E}\times\mathbf{B}$ shear is increased. However, the transport is driven by turbulence and is also proportional to the spectral intensity, and it is well known that $\mathbf{E}\times\mathbf{B}$ shear *suppresses* the turbulence. Therefore, one must in fact consider toroidal momentum transport self-consistently by including the effects of $\mathbf{E}\times\mathbf{B}$ shear suppression on the underlying microturbulence.

We ansatz that for slowly evolving spectra one can model this quenching effect by[29]

$$\varepsilon=\frac{\varepsilon_0}{1+\lambda(\partial\bar{v}_{Ey}/\partial x)^2}, \tag{10}$$

where ε is the intensity of the electrostatic potential and λ is an *ad hoc* saturation parameter. Then, the model equation for the toroidal flow becomes

$$\frac{\partial}{\partial t}\bar{v}_\parallel+\frac{\partial}{\partial x}\left(-[\nu_{\text{neo}}+\nu_1\varepsilon]\frac{\partial}{\partial x}\bar{v}_\parallel-\alpha\varepsilon\left(1-\sigma\frac{\partial}{\partial x}\bar{P}\right)\frac{\partial}{\partial x}\bar{v}_{Ey}\right)=F_\parallel. \tag{11}$$

The heat equation is then

$$\frac{\partial\bar{P}}{\partial t}-\frac{\partial}{\partial x}\left([\chi_{\text{neo}}+\chi_1\varepsilon]\frac{\partial\bar{P}}{\partial x}\right)=H \tag{12}$$

and the particle transport equation is

$$\frac{\partial\bar{n}}{\partial t}-\frac{\partial}{\partial x}\left([D_{\text{neo}}+D_1\varepsilon]\frac{\partial\bar{n}}{\partial x}\right)=S. \tag{13}$$

These should be solved together with radial force balance (8), or in parametrized form,

$$\frac{\partial}{\partial x}\bar{v}_{Ey}=\mu_1\frac{\partial\bar{P}}{\partial x}\frac{\partial\bar{n}}{\partial x}-\mu_2\bar{n}\frac{\partial^2\bar{P}}{\partial x^2}-\beta\bar{v}_\phi-\mu_\beta\frac{\partial}{\partial x}\bar{v}_\phi. \tag{14}$$

We suggest the model given by Eqs. (10)–(14) as a simple, self-consistent transport model, which includes diffusion and an off-diagonal flux of toroidal momentum, as well as density and pressure dynamics, similar, in spirit, to anomalous momentum transport models usually geared towards the NBI-driven case (e.g., Ref. 30). Here, the parameters such as $\nu_{\text{neo}},\nu_1,\alpha,\sigma$, etc., are parametrizations of the corresponding terms in the expressions for the fluxes [i.e., Eqs. (23), (28), and (30)], and the assumed profiles for the sources (S, $F_\parallel$, and H) are given later.

Note that $\sigma\approx v_t\rho_i k_y/2\omega_k^{(r)}$ is negative and $|\sigma|>1$ for the ITG mode, and positive and $|\sigma|<1$ for the electron drift waves as shown in detail later. Hence, while the two terms constituting the torque density term in (11) (i.e., proportional to 1 and $-\sigma\partial P/\partial x$, respectively) add for electron drift waves, they compete for ITG. Nevertheless, the dominant part of the torque density term implies an inward flow for the ITG mode for which α is also negative [i.e., sign $(\alpha\times\sigma\times\partial P/\partial x)=-1$]. For a flow in the negative direction, the conclusion is roughly reversed. Also, various terms in the force balance [i.e., Eq. (14)], that are in the opposite directions for $q'>0$, may act in the same direction for $q'<0$. This suggests, for instance, that apart from the diffusion term (which is an important exception), the discrepancy between corotation and the counter-rotation observed in tokamaks should be roughly reversed in reversed field pinches (RFPs). It should be noted, however, that for RFPs, Maxwell stress driven transport possibly dominates over the Reynolds stress driven flux.[31] In short, the direction of the flux depend on various factors even for this simple model (see Table I for a summary).

III. NUMERICAL RESULTS

The model given in the previous section is a simple transport model. Nevertheless, it is complex enough that analytical solutions are not immediately available. On the other

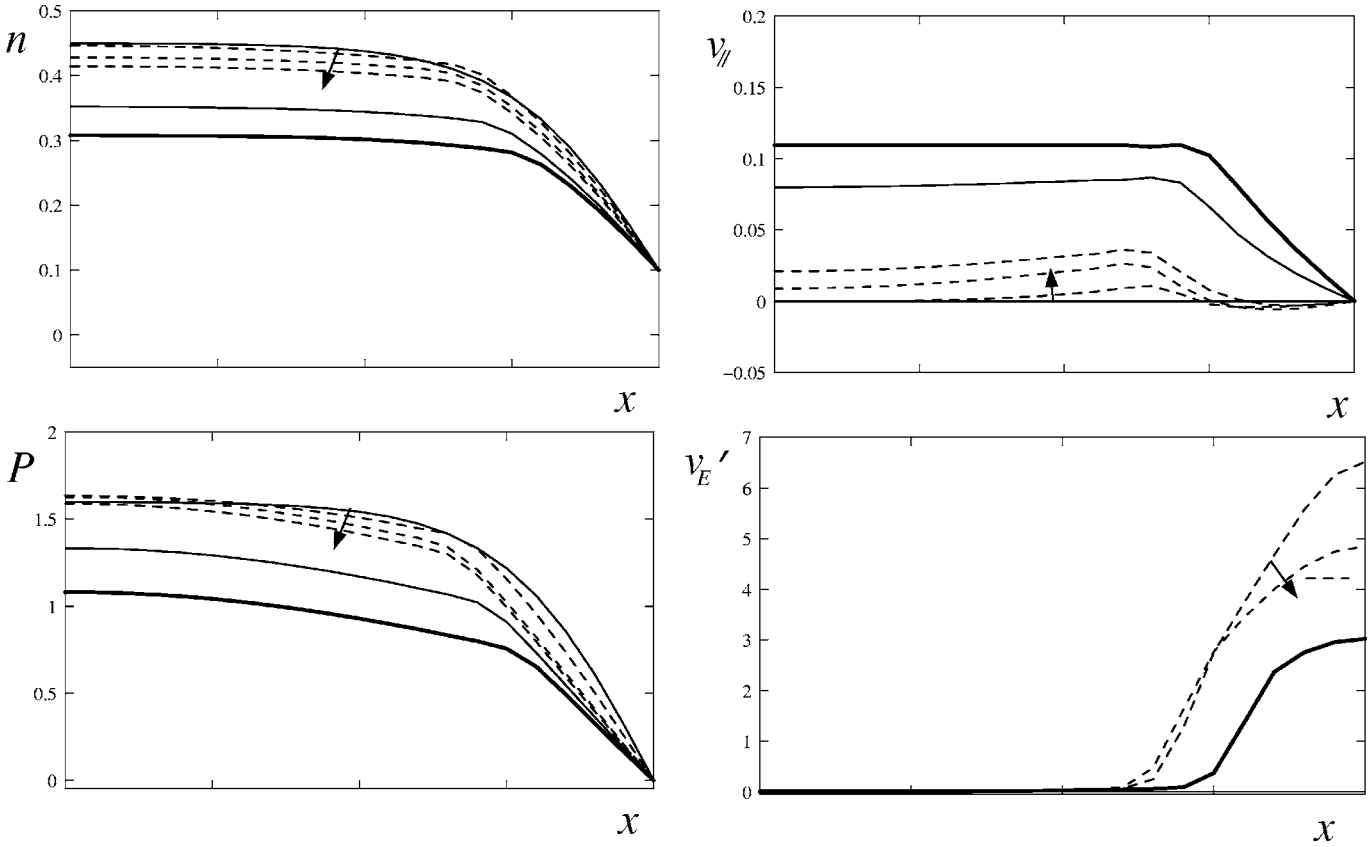

FIG. 4. Profiles of density, pressure, parallel flow, and the radial electric field shear for the $F_{\|}=\mu_2=\mu_\beta=\beta=0$ case. The directions of the evolution of the profiles in time are denoted by the arrows. First few time steps are plotted using dashed lines and the final steady state with a thick solid line. We have plotted intermediate time steps via thin solid lines as long as they can be distinguished from the steady state. Here, the usual normalization is used such that P is in units of n_0T_e, n is in units of n_0, and $v_{\|}$ is in units of c_s. Here, the left-hand side is an open boundary and does not correspond to the actual origin. Therefore, even though a macroscopic scaling (e.g., a) is in fact used, the domain should actually be taken as a finite annulus in the outer core region. Almost all the figures (except some cases in parameter scans) correspond to ITG-like parameters (i.e., $\sigma<0$, $\alpha<0$, etc.).

hand, a three-field system in one dimension is a reasonably simple numerical task for modern computers. The numerical solutions of this model suggest that various steady states (corresponding to the L and H modes) exist, and the system evolves towards one of these steady states depending on the initial conditions. Another observation that can be made from the numerical integration is that the sharp gradients observed in the edge in an H-mode profile can act as a torque density for the toroidal flow, and effectively drive internal rotation, even in the absence of an external source (see, for example, Figs. 4 and 5). Obviously, in the presence of external sources, these too must be included, and can create stronger plasma rotation (see Fig. 6).

The limit $\mu_2=\beta=\nu_\beta=\alpha=0$ corresponds to the Hinton-Staebler model,[29] where conventional heat and particle source profiles are assumed,

$$H=\frac{\partial}{\partial x}\left[2q_a\frac{x}{a}\left(1-\frac{x^2}{2a^2}\right)\right],$$

where q_a and a are coefficients that parametrize the heat source and

$$S=\frac{\partial}{\partial x}[\gamma_a e^{-\eta[n_a(a-x)+g_a(a-x)^2/2]}],$$

where again η, n_a, and $g_a\propto dn/dx|_a$ can be taken as arbitrary parameters that describe the particle source profile. Here, we take the "source" term for toroidal flow to have the same mathematical form as the particle source,

$$F_{\|}=\frac{\partial}{\partial x}[\gamma_v e^{-\eta_v[n_a(a-x)+g_a(a-x)^2/2]}].$$

Note that η_v is an arbitrary form factor that characterizes the spatial extent of this profile. In practice, the scale of this form factor is surely set by either the fueling depth (neutral penetration depth) or the poloidal ion gyroradius (symptomatic of ion neoclassical processes). We note that recent results[32,33] suggest that there are strong neoclassical flows driven in the SOL, which may interact with the core plasma and act as an edge momentum source. It should be noted here that, unlike density and pressure, toroidal flow does not "require" an external source, because the off-diagonal term together with an edge gradient of density and pressure can act as a torque density. In order to demonstrate this we first consider the case where $F_{\|}$ vanishes. The result for the case

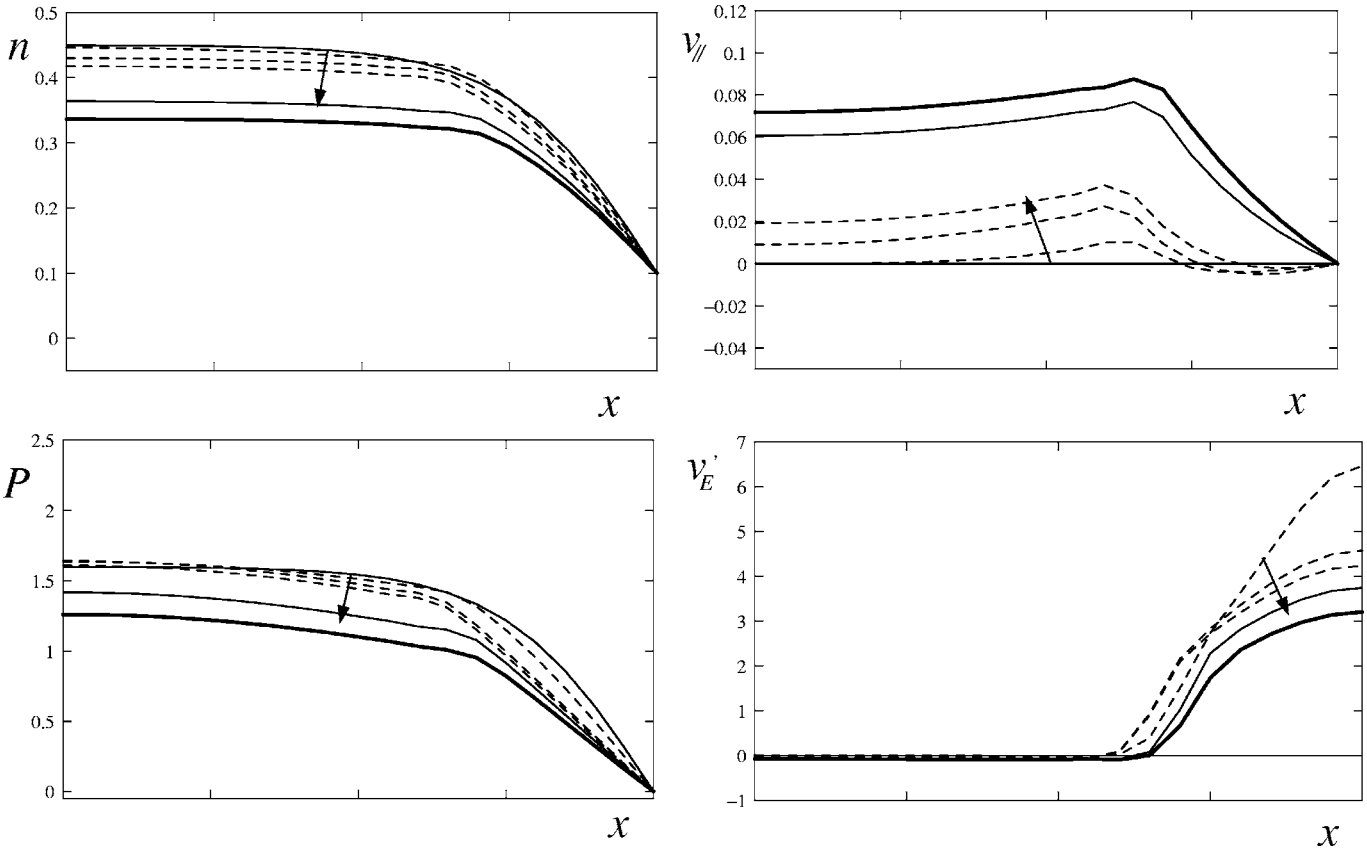

FIG. 5. Profiles of density, pressure, parallel flow, and the radial electric field shear for the $F_{\|}=\mu_2=0$ case, where the effect of toroidal flow is also included in the radial force balance (i.e., $\mu_\beta=\beta=1.0$) resulting in an outward flow proportional to $\bar{v}_\phi$. See Fig. 4 for a key.

$D_0=\chi_0=\mu_1=\beta=\mu_\beta=\gamma_a=\varepsilon_0=1.0$, $\nu_0=0.5$, $\sigma=-2.0$, $\alpha=-1.0$, $\mu_2=0$, $D_1=\chi_1=4.0$, $\nu_1=2.0$, $q_a=3.3$, $\eta=\lambda=10.0$, and $F_{\|}=0$ (i.e., same parameters as in Ref. 29) is shown in Fig. 4. Note that in this case the generated flow is about $0.1c_s$, which is not extremely strong, but the resulting flow depends on input parameters and one can get higher values by using different parameters. Thus, parameter scans of parallel velocity at $x=0$ versus α, σ, v_0 (i.e., flow at the boundary), and γ_v was performed and the results are plotted in Fig. 7. Note that both Figs. 7(c) and 7(d) display bifurcation behavior. In this simple model, the bifurcation in velocity is always associated with the bifurcations in P and n as well. Thus, the jump seen in Figs. 7(c) and 7(d) correspond to switching from L-mode-type profiles to H-mode-type profiles as we go from right to left. Note that negative values of both α and σ correspond to the ITG-type parameter regime.

The case $\gamma_v=1$ (i.e., $F_{\|}\neq 0$) is shown in Fig. 6. Not unexpectedly, the flow generated with the strong edge momentum source is considerably larger than the case without the edge source. Note that the $\mu_2\neq 0$ case is numerically challenging when $F_{\|}=0$, because of the "corner" from the barrier. Nevertheless, we have done the case $\mu_2=\mu_1=1.0$, and the result is depicted in Fig. 8. The pressure "curvature" term (i.e., the $\partial^2 P/\partial x^2$ term in the radial force balance), seems to affect the background profiles of pressure and density substantially, thus resulting in a very different velocity profile (almost linear in x). This is of course only a single case, and needs to be studied by changing the parameters. Paradoxically though, in the steady state obtained when we include the curvature term, the curvature term seems to be negligible. But when it is neglected, "the corner" appears and is not negligible. Also, the E_r' profile changes substantially, and it seems that the open-end boundary on the left starts to play an important role in the dynamics, which could be an artifact of the numerical setup.

As shown in this section, parameter scans of numerical integrations of the system of Eqs. (10)–(14) reveal that some rotation can be generated via the torque density term. Nevertheless, an edge source, or a boundary condition, would help explain the observed rotation speeds. Hence, SOL flows should be studied as feasible candidates for a better quantitative modeling of the edge momentum source.

IV. GYROKINETIC DERIVATION

A. Two-scale kinetic evolution

We assume the fluctuations evolve at a fast time scale and are described by the gyrokinetic equation,

$$(\bar{D}_t + v_\| \nabla_\|)\tilde{g} = J_0\left(\frac{k_\perp v_\perp}{\Omega_i}\right)\left[\bar{D}_t\left(\frac{e\Phi}{T_i}\right) + \Omega_i \rho_i^2 \frac{\partial}{\partial y}\left(\frac{e\Phi}{T_i}\right) L_f^{-1}(x,v)\right]\langle f\rangle, \tag{15}$$

where $\bar{D}_t=\partial_t+\bar{\mathbf{v}}_0\cdot\boldsymbol{\nabla}$ is the mean convective derivative, which includes the mean $\mathbf{E}\times\mathbf{B}$ flow as well as any other overall

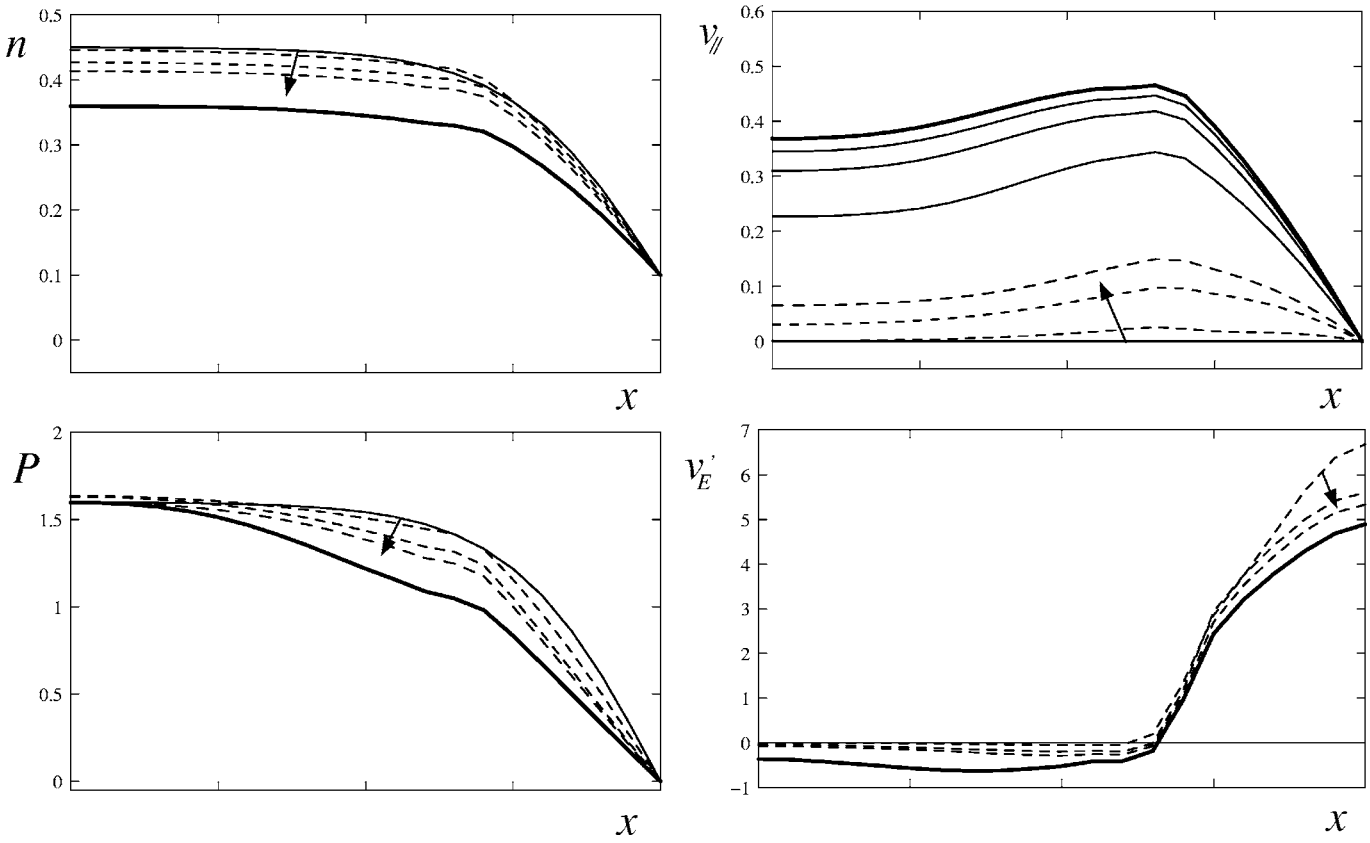

FIG. 6. Profiles of density, pressure, parallel flow, and the radial electric field shear for the $\mu_2=\mu_\beta=\beta=0$ case with an edge momentum source similar to particle source ($\gamma_v=1.0$ case). See Fig. 4 for a key.

drifts that may exist. Here, Ω_i is the ion cyclotron frequency, ρ_i is the ion Larmor radius, Φ is the electrostatic potential, e is the magnitude of fundamental charge, T_i is the ion temperature, $\tilde{g}$ is the nonadiabatic part of the fluctuation distribution (i.e., $\tilde{f}=-e/T_i\tilde{\Phi}\langle f\rangle+\tilde{g}$, where $\tilde{f}$ is the total fluctuation distribution), $\langle f\rangle$ is the background Maxwellian distribution, shifted by a mean toroidal flow $\bar{v}_\parallel$, J_0 is the Bessel function of the first kind of the order 0, and $L_f^{-1}(x,v)$ is the length scale for the radial gradient of this background distribution:

$$L_f^{-1}(x,v) \equiv \frac{1}{\langle f\rangle}\frac{d\langle f\rangle}{dr} = \frac{1}{\bar{n}}\frac{d\bar{n}}{dx}\left[1-\eta_i\left(3/2-\frac{v_\perp^2}{2v_{ti}^2}-\frac{(v_\parallel-\bar{v}_\parallel(x))^2}{2v_{ti}^2}\right)\right]+\frac{(v_\parallel-\bar{v}_\parallel(x))}{v_{ti}^2}\frac{d\bar{v}_\parallel(x)}{dx}.$$

On the other hand, mean flows evolve on a slower time scale and can be adequately described by the drift-kinetic equation, driven quasilinearly by the fluctuations,

$$\frac{\partial}{\partial t}\langle f_s\rangle+\langle\tilde{\mathbf{v}}_E\cdot\boldsymbol{\nabla}_\perp\tilde{f}_s\rangle+\frac{q_s}{m_s}\left\langle\tilde{E}_\parallel\frac{\partial}{\partial v_\parallel}\tilde{f}_s\right\rangle=0, \tag{16}$$

where $s=\{i,e\}$ corresponds to ions and electrons, respectively, $\tilde{\mathbf{v}}_E$ is the fluctuating $\mathbf{E}\times\mathbf{B}$ flow, and $\tilde{E}_\parallel$ is the fluctuating parallel electric field.

In order to construct a self-consistent quasilinear model of turbulent evolution of toroidal momentum, we first compute the moments of the drift kinetic equation for ions and electrons. Together with the quasineutrality condition, these give the evolution of mean density, mean toroidal momentum, and mean pressure, evolving under the action of turbulent stresses. Then, we use the solution of the gyrokinetic equation, assuming that the background Maxwellian distribution is a function of the mean density, temperature, and parallel flow, and compute the first three moments of the gyrokinetic distribution. These moments yield the fluctuation fields that appear in the expressions for the Reynolds stresses. Then computing the Reynolds stresses in terms of the mean fields gives a self-consistent model for the transport of these mean fields.

B. Moments of the drift kinetic equation

We start with the zeroth moment of (16), which gives the equation for the mean density evolution,

$$\partial_t\bar{n}+\partial_x\langle\tilde{v}_{Ex}\tilde{n}\rangle=0. \tag{17}$$

Then, we consider the $v_\parallel$ moment, which gives the equation for parallel momentum,

$$\frac{\partial}{\partial t}(m\bar{n}\bar{v}_\parallel)+m[\bar{n}\,\boldsymbol{\nabla}\cdot\langle\tilde{\mathbf{v}}_E\tilde{v}_\parallel\rangle+\bar{v}_\parallel\,\boldsymbol{\nabla}\cdot\langle\tilde{\mathbf{v}}_E\tilde{n}\rangle]=0. \tag{18}$$

Here, we also used the quasineutrality condition, which cancels the effect of the mean "stress" originating from the parallel velocity space nonlinearity. An immediate observation that can be made from (18) is that mean momentum can be transported either by the Reynolds stress term (i.e., $\langle\tilde{\mathbf{v}}_E\tilde{v}_\parallel\rangle$), or convectively via the particle flux (i.e., $\langle\tilde{\mathbf{v}}_E\tilde{n}\rangle$). Similarly,

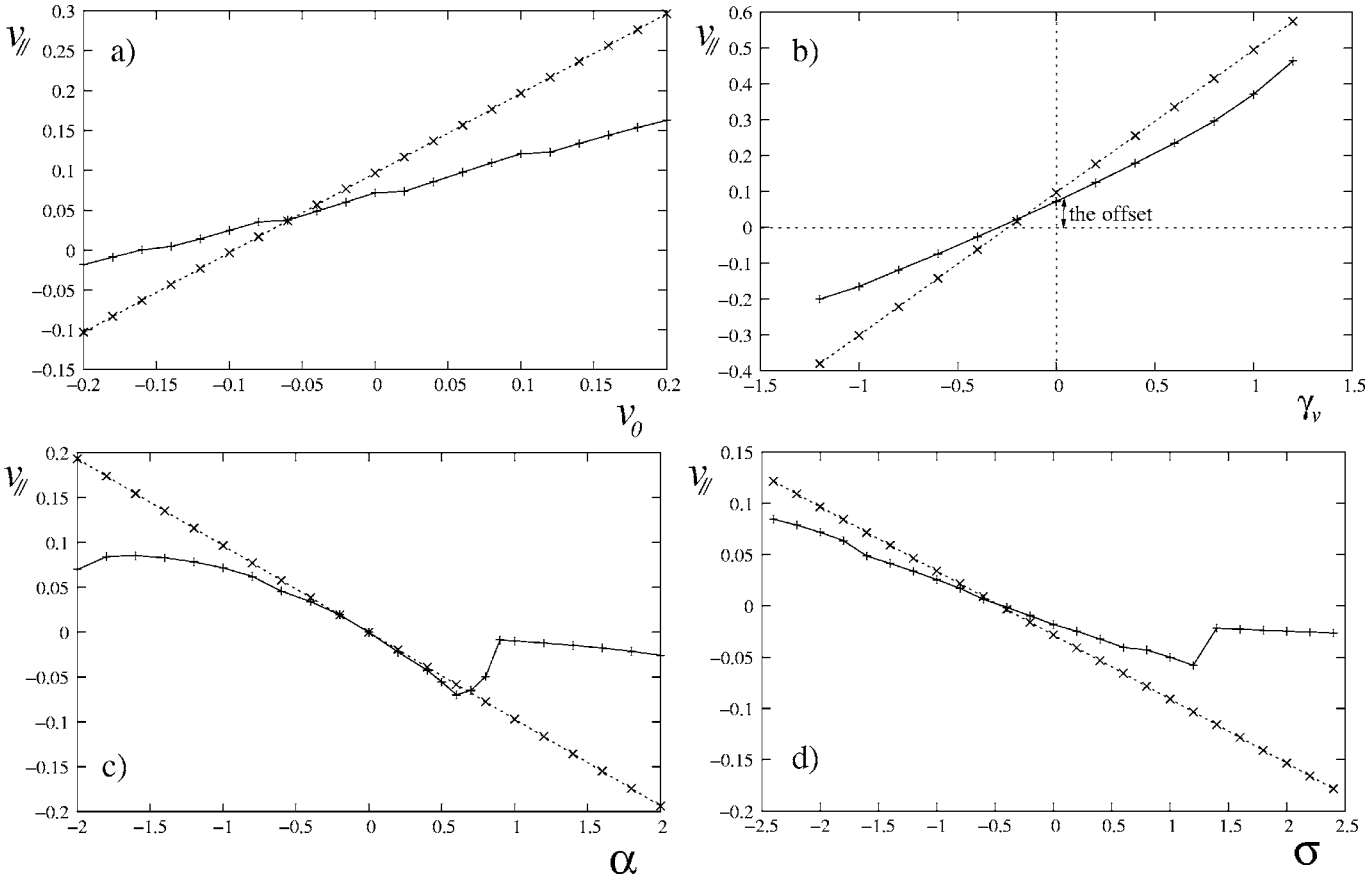

FIG. 7. Scaling of toroidal flow velocity with parameters (a) v_0, the value of $v_\parallel$ at the right hand boundary (i.e., boundary condition at $x=a$); (b) γ_v, the external momentum input; (c) α; and (d) σ. In all the figures, the dashed lines correspond to the case $\mu_\beta=\beta=0$, whereas the solid lines are $\mu_\beta=\beta=1$. Here $v_\parallel$ is the parallel flow velocity normalized to c_s at the left boundary, which is open. Note that this point does not always correspond to the maximum of the velocity profile especially when the radial momentum flow terms are turned on (i.e., $\beta=1$).

the equation for the evolution of mean pressure (which is assumed to be isotropic) follows from taking the second moment $(v_\parallel-\bar{v}_\parallel)^2$ and has the form,

$$\frac{\partial}{\partial t}\bar{P}+\nabla\cdot[\bar{n}\langle\tilde{\mathbf{v}}_E\tilde{T}\rangle+\bar{T}\langle\tilde{\mathbf{v}}_E\tilde{n}\rangle]=0.$$

Pressure, too, can be transported either via the heat flux (involving $\tilde{T}$) or convectively, by the particle flux. Notice that by taking the difference between $v_\parallel$ moments [instead of the sum, which leads to (18)] we also obtain the equation,

$$\frac{\partial}{\partial t}\bar{J}_\parallel+e\langle\tilde{E}_\parallel\tilde{n}\rangle=0 \tag{19}$$

within this framework. This identifies yet another path to symmetry breaking, namely via current generation by parallel electric field fluctuations. Here the waves that are antiparallel to the generated current (i.e., parallel to the "mean electron flow") grow, while the waves parallel to the current (antiparallel to the electron flow) damp. This, too, creates a difference in wave population densities. Since we expect this mechanism to be weaker than the electric field shear mechanism, here we focus only on the latter.

It should be noted, however, that experimental diagnostics usually give information about the ion flow instead of the "fluid flow" commonly used in theoretical formulation. If formulated using the ion flow, part of the $e\langle\tilde{E}_\parallel\tilde{n}\rangle$ term would appear in the parallel ion momentum equation and would cancel a certain part of the flux term in Eq. (18).

C. Moments and stresses from gyrokinetics

In order to compute the stress terms, we need to compute the first three moments (i.e., n, v, and P) using (15) and (16). Here we assume temporal scale separation, so that the fluctuations have enough time to form semistationary eigenmodes on the time scale at which the mean flows evolve. This allows us to solve simply for $\tilde{g}$ from (15) in terms of $\langle f\rangle$, which in turn allows us to compute moments of fluctuation quantities, i.e.,

$$\tilde{n}^{(i)}_{k,\omega}=-\bar{n}\frac{e\tilde{\Phi}_{k,\omega}}{T}+2\pi\int v_\perp dv_\perp\int dv_\parallel J_0\left(\frac{k_\perp v_\perp}{\Omega}\right)\tilde{g}(k,\omega). \tag{20}$$

Performing the integrals over the velocity space, we obtain

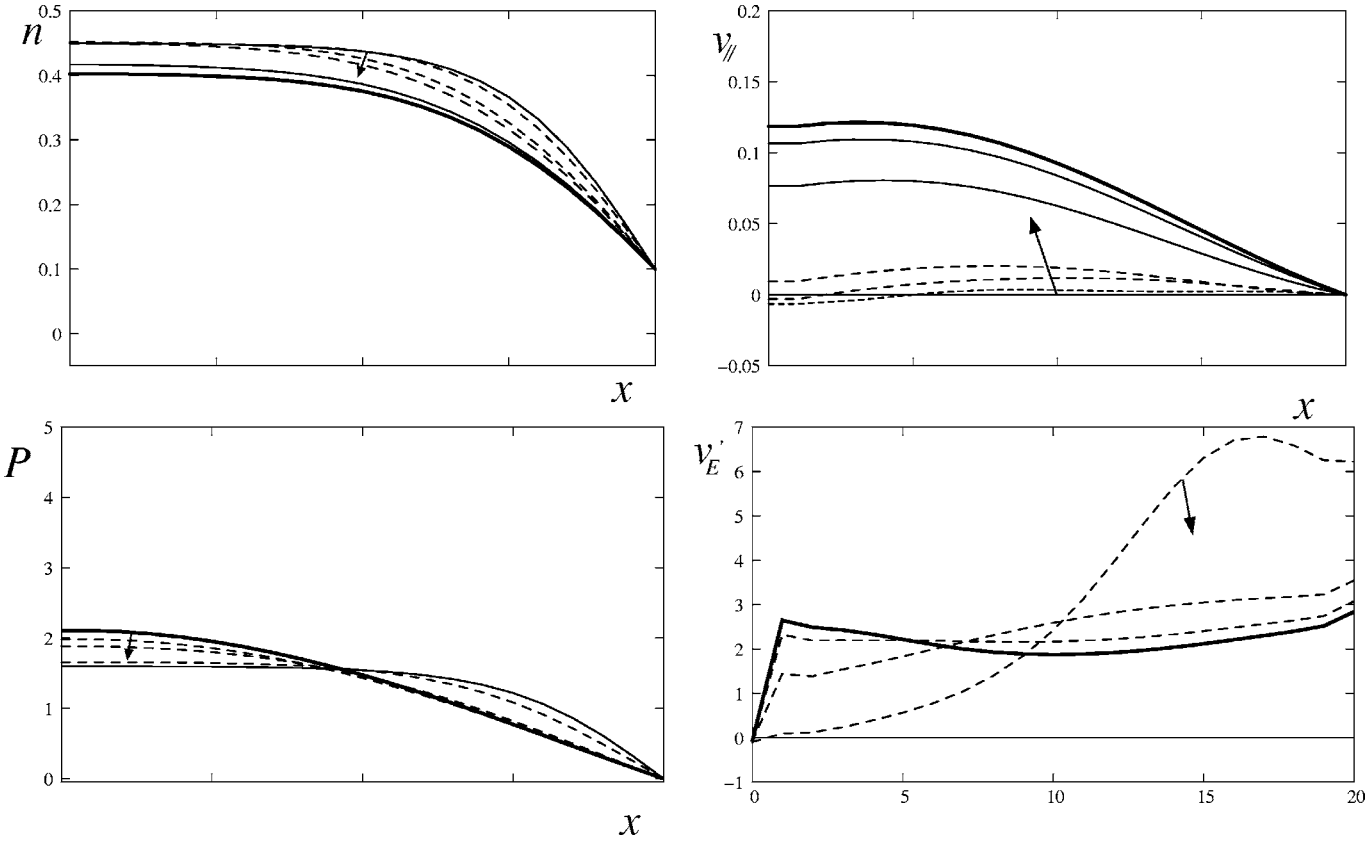

FIG. 8. The case with $\mu_1=\mu_2=1.0$ and $F_\parallel=\mu_\beta=\beta=0$. See Fig. 4 for a key.

$$\tilde{n}_{k,\omega}^{(i)} \approx -\frac{e\bar{n}}{T_i}\tilde{\Phi}_{k,\omega}\left[1+\frac{\zeta}{\bar{\omega}}\Gamma_0\left\{\left(\bar{\omega}-\omega_{*i}\left[1-\eta_i\left(\frac{1}{2}+b-\frac{b\Gamma_1}{\Gamma_0}-\zeta^2\right)-\sqrt{2}\zeta\frac{L_n}{v_{ti}}\frac{d\bar{v}_\parallel}{dx}\right]\right)Z(\zeta)+\omega_{*i}\left(\sqrt{2}\frac{L_n}{v_{ti}}\frac{d\bar{v}_\parallel}{dx}-\eta_i\zeta\right)\right\}\right], \tag{21}$$

where $L_n=-d\ln n/dx$, $\omega_{*i}=-\Omega_i\rho_i^2L_n^{-1}k_y$, $\bar{\omega}=\omega-k_y\bar{v}_{Ey}(x)$, $\eta_i=d\ln T/d\ln n$, $\zeta=\bar{\omega}/\sqrt{2}k_\parallel v_{ti}$, $b=k_\perp^2\rho_i^2$, $Z(\zeta)$ is the plasma dispersion function, and $\Gamma_n=I_n(b)e^{-b}$, where $I_n(b)$ is the modified Bessel function. Notice that the only term that is odd with respect to ζ is the coefficient of flow shear [since $Z(\zeta)$ is odd] and that all the other terms are even.

The fluid limit of (21) can be obtained by taking $\zeta^{-2}\sim b\sim k_yx/\omega_{*e}dv_{Ey}/dx\sim\zeta^{-1}L_n/v_{ti}dv_\parallel/dx\sim\delta_k\sim O(\epsilon)$ and neglecting higher-order terms, to obtain

$$\tilde{n}_i \approx \frac{e\bar{n}}{T_e}\tilde{\Phi}\frac{1}{\bar{\Omega}}\left[1+(\bar{\Omega}+K)\frac{\tau\zeta^{-2}}{2}-\frac{L_n}{v_{ti}}\frac{d\bar{v}_\parallel}{dx}\frac{\zeta^{-1}}{\sqrt{2}}-b\tau(\bar{\Omega}+K)-\frac{x}{\rho_i}\frac{L_n}{v_{ti}}\frac{d\bar{v}_{Ey}}{dx}\right], \tag{22}$$

where $\bar{\Omega}\equiv\bar{\omega}/\omega_{*e}$, $K=(1+\eta_i)/\tau$, and $\tau=T_e/T_i$. Notice that the $\mathbf{E}\times\mathbf{B}$ shear enters at the lowest order. This form, which we argue is the correct fluid limit, is in fact slightly different from the form one would get if one took the fluid limit first and then tried to incorporate the effects of the lowest-order sheared $\mathbf{E}\times\mathbf{B}$ flow into that fluid calculation.

Of course, for the particle flux, $\tilde{n}_i$ is not really needed, since it is possible to write simply

$$\langle\tilde{v}_{Ex}\tilde{n}_i\rangle=\mathrm{Re}\sum_k iL_n\omega_{*e}\frac{e\tilde{\Phi}_{-k}}{T_e}\tilde{n}_k^{(e)}, \tag{23}$$

due to quasineutrality. Note that this form is also valid in the fluid limit, and that it implies that the electron response determines the particle flux.

We also need the $(v_\parallel-\bar{v}_\parallel)$ moment of the fluctuation distribution in order to compute $\langle\tilde{v}_{Ex}\tilde{v}_\parallel\rangle$, since

$$\bar{n}\tilde{v}_\parallel=2\pi\int v_\perp dv_\perp\int(v_\parallel-\bar{v}_\parallel)dv_\parallel J_0\left(\frac{k_\perp v_\perp}{\Omega}\right)\tilde{g},$$

which gives

$$\tilde{v}_\parallel=-\sqrt{2}v_{ti}\frac{\Gamma_0\zeta}{\Omega}\left[\left(\Omega\tau+1-\eta\left[\frac{1}{2}-b\frac{(\Gamma_0-\Gamma_1)}{\Gamma_0}-\zeta^2\right]-\sqrt{2}\frac{\zeta L_n}{v_{ti}}\frac{d\bar{v}_\parallel}{dx}\right)[1+\zeta Z(\zeta)]+\frac{\eta}{2}\right]\frac{e\tilde{\Phi}}{T} \tag{24}$$

after integrations. Notice that if one computes the $v_\parallel$ moment [instead of $(v_\parallel-\bar{v}_\parallel)$], which would correspond to $\tilde{nv}_\parallel$ (instead of $\bar{n}\tilde{v}_\parallel$), and computes the Reynolds stress using that expression, one finds

$$\langle \tilde{v}_{\mathrm{Ex}} \tilde{n} \tilde{v}_{\parallel} \rangle = \bar{n} \langle \tilde{v}_{\mathrm{Ex}} \tilde{v}_{\parallel} \rangle + \bar{v}_{\parallel} \langle \tilde{v}_{\mathrm{Ex}} \tilde{n} \rangle + \langle \tilde{v}_{\mathrm{Ex}} \tilde{n} \tilde{v}_{\parallel} \rangle. \tag{25}$$

We drop the last term, which can be identified as the triplet contribution to the momentum flux, since it requires a higher-order closure. Note that the triplet term is similar to that which is calculated in the theory of "turbulence spreading."[34] This term could be important in regions of strong turbulence or in regimes where competing quasilinear contributions cancel.

Note that there appears a term in (25) that has the form of a "pinch term" (i.e., proportional to $\bar{v}_{\parallel}$). Comparing with (18), we can identify this term as the convective momentum flux term. In other words, a substantial part of the "momentum pinch" that was discovered in Ref. 25 is merely the particle pinch, transporting momentum convectively (since the particles that are transported possess average momentum). We deem it important to distinguish this effect from an off-diagonal inward flux appearing from the Reynolds stress.

Using (24) to compute the Reynolds stress term, we then obtain

$$\langle \tilde{v}_{\mathrm{Ex}} \tilde{v}_{\parallel} \rangle = -\,\mathrm{Re} \sum_k i\sqrt{2} v_{ti} L_n \frac{\omega_{*e}^2}{\omega} \Gamma_0 \zeta \left[\left(\Omega\tau + 1 - \eta \left[\frac{1}{2} - b\frac{(\Gamma_0 - \Gamma_1)}{\Gamma_0} - \zeta^2 \right] - \sqrt{2}\frac{\zeta L_n}{v_{ti}} \frac{d\bar{v}_{\parallel}}{dx} \right) \times [1 + \zeta Z(\zeta)] + \frac{\eta}{2} \right] \left| \frac{e\tilde{\Phi}}{T} \right|^2. \tag{26}$$

Note that this concludes the derivation of (9) [see the discussion in Sec. I after (9)].

If we take the fluid limit of (24), we get

$$\tilde{v}_{\parallel} = v_{ti} \frac{1}{\bar{\Omega}} \frac{e\tilde{\Phi}}{T_e} \left[(\bar{\Omega} + K) \frac{\tau\zeta^{-1}}{\sqrt{2}} - \frac{L_n}{v_{ti}} \frac{d\bar{v}_{\parallel}}{dx} \right] + \tilde{v}_{\parallel}^{(\text{higher order})}, \tag{27}$$

where the higher-order terms that have been neglected are presented in the Appendix. The Reynolds stress can be computed using the expressions for the fluid limit, and is

$$\langle \tilde{v}_{\mathrm{Ex}} \tilde{v}_{\parallel} \rangle = \mathrm{Re} \sum_k i c_s^2 \left[\frac{c_s \rho_s k_{\parallel} k_y}{\omega} \left(1 - \frac{c_s k_y}{\omega} \frac{\rho_s}{P_e} \frac{d\bar{P}}{dx} \right) - \frac{\rho_s^2 k_y^2}{\omega} \frac{d\bar{v}_{\parallel}}{dx} \right] \left| \frac{e\tilde{\Phi}}{T_e} \right|^2, \tag{28}$$

which is, in fact, the same as (5) (note that $\omega = \omega^{(r)} + i\gamma$).

Thus, again we find that, as long as the spectrum is symmetric, the nondiffusive terms in Eq. (28) vanish. Therefore, a mechanism for symmetry breaking must be identified in order to produce and account for the imbalance between the sound waves propagating in opposite directions. We argued that the effect of a poloidal $\mathbf{E}\times\mathbf{B}$ sheared flow on the eigenmode is sufficient to explain the appearance of a net wave momentum.

The next moment in the hierarchy is pressure. Here, using isotropic pressure $\tilde{P} = 3\tilde{P}_{\parallel} = m\langle (v_{\parallel} - \bar{v}_{\parallel})^2 \rangle = \bar{n}\tilde{T} + \tilde{n}\bar{T}$, we write

$$\bar{n}\tilde{T} = 2\pi \int v_{\perp} dv_{\perp} \int dv_{\parallel} 3 \left\{ \frac{m}{3} (v_{\parallel} - \bar{v}_{\parallel})^2 - \bar{T}_{\parallel} \right\} \tilde{g},$$

so that

$$\tilde{T} = -\,T_i \frac{e\tilde{\Phi}}{T_e} \Gamma_0(b) \frac{\zeta}{\Omega} \left[\left\{ \tau\Omega + 1 - \eta_i \left(\frac{1}{2} + b - \frac{b\Gamma_1}{\Gamma_0} - \zeta^2 \right) - \frac{\sqrt{2}}{v_{ti}} \zeta L_n \frac{d\bar{v}_{\parallel}}{dx} \right\} [2\zeta + (2\zeta^2 - 1) Z(\zeta)] \right]. \tag{29}$$

The fluid limit for the fluctuating temperature is

$$\tilde{T} \approx -\,T_i \frac{\omega_{*e}}{\omega} L_n \left(\frac{1}{T_i} \frac{dT}{dx} \right) \left(\frac{e\tilde{\Phi}}{T_e} \right),$$

where again the higher-order terms, which have been neglected, are given in the Appendix. In order to apply our strategy, we also need to compute the heat flux,

$$\langle \tilde{v}_{\mathrm{Ex}} \tilde{T}_i \rangle = \mathrm{Re} \sum_k -iT_i \frac{L_n \omega_{*e}^2}{\omega} \left(\frac{L_n}{T_i} \frac{dT}{dx} \right) \left| \frac{e\tilde{\Phi}}{T_e} \right|^2 = -\,\mathrm{Re} \sum_k ic_s^2 \frac{\rho_s^2 k_y^2}{\omega} \left(\frac{dT}{dx} \right) \left| \frac{e\tilde{\Phi}}{T_e} \right|^2, \tag{30}$$

which also has the form of a turbulent diffusion.

D. Eigenmode equation

A fairly general form of the eigenmode equation for the fluctuations can be obtained using (21), quasineutrality, and a simple electron response such as

$$\frac{\tilde{n}_{ek,\omega}}{\bar{n}} = \frac{e}{T_e} (1 - i\delta_{k,\omega}) \tilde{\Phi}_{k,\omega}. \tag{31}$$

Upon substitution, this gives

$$\left\{ \Omega(1 - i\delta_k + \tau) + \Gamma_0 \zeta Z(\zeta) \left[\Omega\tau + 1 - \eta_i \left[\frac{1}{2} + b - \frac{\Gamma_1}{\Gamma_0} b - \zeta^2 \right] - \sqrt{2}\zeta \frac{L_n}{v_{ti}} \frac{d\bar{v}_{\parallel}}{dx} \right] - \Gamma_0 \zeta \left(\sqrt{2} \frac{L_n}{v_{ti}} \frac{d\bar{v}_{\parallel}}{dx} - \eta_i \zeta \right) \right\} \frac{e\tilde{\Phi}_{k,\omega}}{T_e} = 0, \tag{32}$$

which should be interpreted as an operator equation because of its dependence on $\bar{b} \to \tau^{-1}\rho_s^2[k_y^2 - \partial_x^2]$, both explicitly and via the terms involving $\Gamma_n = \Gamma_n(\bar{b})$. Note that $\delta_k \ll 1$, since electrons are nearly adiabatic. In (32) the effect of $\bar{v}_{\parallel}'(x)$ is shown explicitly, however, the effect of $\mathbf{E}\times\mathbf{B}$ shear enters indirectly via the $\Omega = (\omega - k_y \bar{v}_{Ey}(x))/\omega_{*e}$ term (i.e., via a differential Doppler shift). Note that this form agrees well with that in Ref. 35.

E. Fluid limit with E×B shear

The general form of the eigenmode equation in (32) is not easily tractable. Instead, it is useful to consider the fluid limit, which can be obtained either by directly taking the fluid limit of (32), or using (22), (31), and the quasineutrality condition. This gives

$$\rho_s^2 \frac{\partial^2 \Phi}{\partial x^2} + Q(k,x,\omega)\Phi = 0, \tag{33}$$

where

$$Q(k,x,\omega) = -\rho_s^2 k_y^2 + \frac{1-\Omega(1-i\delta_k)}{\Omega+K} + \frac{1}{(\Omega+K)}\left(\frac{L_n}{c_s}\right) \times \left[\frac{d\bar{v}_{Ey}}{dx} - \frac{s}{\Omega}\frac{d\bar{v}_{\|}}{dx}\right]\frac{x}{\rho_s} + \frac{s^2}{\Omega^2}\frac{x^2}{\rho_s^2}, \tag{34}$$

and where $s=L_n/L_s$ and $K=(1+\eta_i)/\tau$. Note that this has exactly the same form as the eigenmode equation in Ref. 2, where $J^{1/2} \equiv L_n/c_s d\bar{v}_{\|}/dx$ is replaced by $L_n/c_s(d\bar{v}_{\|}/dx - \Omega/s d\bar{v}_{Ey}/dx)$. Thus, we have the same dispersion relation, eigenmodes, etc.

Note that the form of the eigenmode equation as given by Eqs. (33) and (34) suggests that the shift can be caused by $d\bar{v}_{\|}/dx$ as well as $d\bar{v}_{Ey}/dx$. In the past, some authors suggested that this may supply the required symmetry-breaking mechanism and "explain" spontaneous rotation.[22,21] However, when the $d\bar{v}_{\|}/dx$ term in (34) is kept, it can be shown that the shift generated by this term yields a "diffusive term" in the momentum equation (i.e., naturally proportional to $d\bar{v}_{\|}/dx$). It is in fact possible that this term might have a positive sign (i.e., competing with the Fick's law), however, since it has a diffusive form, it simply ends up slightly modifying the effective "diffusion coefficient."

Since (34) has the form $Q(k,x,\omega) \equiv Ax^2 - Bx + C$, the dispersion relation can be obtained from it by requiring $\ell + 1/2 = -i/2\sqrt{A}(C - B^2/4A)$, which gives

$$\Omega^2(1+\rho_s^2k^2 - i\delta_k) + \Omega(K\rho_s^2k^2 - 1 + is(2\ell+1)) + is(2\ell+1)K = -\frac{1}{4}\left(\frac{\Omega}{\Omega+K}\right)\left(\frac{L_n}{c_s}\right)^2\left(\frac{d\bar{v}_{\|}}{dx} - \frac{\Omega}{s}\frac{d\bar{v}_{Ey}}{dx}\right)^2. \tag{35}$$

Notice that the analysis from this point on depends on what kind of solutions are considered. For instance, if $\gamma \ll \omega$ we have the electron drift wave branch, which gives oscillatory solutions, where the shape of the envelope is determined either by the effects of Landau damping or by the weak linear growth (whichever is stronger).

On the other hand, for the so-called η_i branch we have $\omega \sim O(\epsilon)$, and the linear growth dominates, resulting in a bell-shaped eigenmode. Let us consider these two cases in reverse order, since the latter seems to be simpler.

F. Shift of the spectra

The existence of nondiffusive terms in the Reynolds stress depends crucially on $\langle k_y k_{\|} \rangle$. This is in fact determined by the shift of the fluctuation intensity, and not the eigenmode. Thus, we need to compute the shift of the fluctuation intensity for various branches of the dispersion relation.

1. η_i branch

If we consider the limit $\Omega \sim s \sim O(\epsilon)$, expanding the dispersion relation and iterating for the case with weak sheared flow and finite Larmor radius (FLR) effects, we get

$$\Omega \sim is\left(K + \rho_s^2k^2K^2 + \frac{L_n^2/c_s^2}{4K}\left[\left(\frac{d\bar{v}_{\|}}{dx} - iK\frac{d\bar{v}_{Ey}}{dx}\right)^2\right]\right)$$

for this branch. Note that without sheared flows, this branch is essentially purely imaginary. We take the growing mode

$$\gamma \approx \omega_{*e} sK$$

to be positive by convention. In this limit Q becomes

$$Q \sim -\rho_s^2k_y^2 + \frac{1-iK}{K} - \frac{i}{K^2}\left(\frac{L_n}{c_s}\right)\left[iK\frac{d\bar{v}_{Ey}}{dx} - \frac{d\bar{v}_{\|}}{dx}\right]\frac{x}{\rho_s} - \frac{1}{K^2}\frac{x^2}{\rho_s^2},$$

$$\Phi_\ell(x) = A_\ell e^{-1/2\Delta_k^2(x-\xi-ix_0)^2} H_\ell\left(\frac{(x-\xi-ix_0)}{\Delta_k}\right),$$

where

$$\Delta_k^2 = K\rho_s^2 \quad \frac{x_0}{\rho_s} = \frac{L_n}{2c_s}\frac{d\bar{v}_{\|}}{dx}$$

and

$$\frac{\xi}{\rho_s} = K\frac{L_n}{2c_s}\frac{d\bar{v}_{Ey}}{dx}.$$

This implies that the spectrum (for $\ell=0$, which accounts for the main contribution) is given by

$$|\Phi_0(x)|^2 = \alpha e^{-1/\Delta_k^2(x-\xi)^2},$$

where the effect of the toroidal sheared flow has been absorbed into the normalization constant A_ℓ, and ξ corresponds to the shift of the spectrum. In particular, note that the symmetry-breaking spectral shift is directly proportional to the electric field shear. Thus, for the η_i limit, the shift in the eigenmode occurs "only" via the $\mathbf{E}\times\mathbf{B}$ sheared flow. Note that this actually agrees with the expression in Ref. 2 [i.e., the shift in Eq. (10) in Ref. 2 becomes purely imaginary in the absence of electric field shear, given our assumptions].

2. Drift wave branch

The drift wave eigenmode for the case $\omega \gg \gamma$ can be localized in two ways: Due to (a) finite growth rate γ or (b) Landau damping. Depending on which one of these effects is stronger, the shape of the eigenmode is determined by that effect. We consider these two cases in sequence.

a. Localization via finite γ If we consider the case $\omega \gg \gamma$ for the dispersion relation (35) with weak flow shear, we obtain

$$\Omega \approx \frac{(1-K\rho_s^2k^2)}{(1+\rho_s^2k^2)}.$$

In this case, both the toroidal and the poloidal sheared flows will act to shift the eigenmode, but the eigenmode is not localized without Landau damping or growth. Thus, one has to include higher-order effects. If we simply iterate the dispersion relation, at the first iteration we obtain

$$\Omega \sim \frac{1}{1+\rho_s^2k^2} + \frac{i\text{sign}[\omega_{*e}]}{(1+\rho_s^2k^2)}\left| sK - \frac{\delta_k}{(1+\rho_s^2k^2)} \right|, \tag{36}$$

which has the basic form that we want. Further iteration is not necessary since the effect of the sheared flows on the linear frequencies can be neglected when computing the shift in the eigenmode. Notice that the real part of $\Omega_r=\omega_r/\omega_{*e}$ is positive, but the imaginary part has the sign of ω_{*e}, so that γ itself, written in this form, is also positive.

However, expanding (32) with the assumptions $\gamma/\omega \sim \rho_s^2k^2 \sim k_\parallel^2 v_{ti}^2/\omega^2 \sim O(\epsilon)$ and taking the fluid limit, is not sufficient for localization and one should include higher-order corrections in γ/ω,

$$\begin{aligned} Q \sim & -\rho_s^2k_y^2 + \frac{1-\Omega_r}{\Omega_r+K} - i\frac{\Gamma(1+K)}{(\Omega_r+K)^2} \\ & - \frac{1}{(\Omega_r+K)}\left(1 - i\frac{\Gamma}{(\Omega_r+K)}\right)\left(\frac{L_n}{c_s}\right)\frac{d\bar{v}_{Ey}}{dx}\frac{x}{\rho_s} \\ & + \frac{s^2x^2}{\Omega_r^2\rho_s^2}\left(1 - 2i\frac{\Gamma}{\Omega_r}\right). \end{aligned}$$

Here the effect of toroidal sheared flow has been neglected because of the factor s/Ω_r in front of it. This has the generic form with all coefficients complex, hence the solution has the general form,

$$\begin{aligned} \Phi_\ell(x) = & A_\ell e^{-i1/2\Delta_k^2\text{sign}(\text{Im }\Delta_k^2)(x-x_0)^2} \\ & \times H_\ell\left(\frac{e^{i\text{sign}(\text{Im }\Delta_k^2)\pi/4}}{\Delta_k}(x-x_0)\right), \end{aligned} \tag{37}$$

where the boundary condition is taken to be a decaying envelope at infinity. Note that one can further impose "the outgoing wave" condition to determine the phase of the eigenmode. Here we only need the intensity. The coefficients in (37) are

$$\frac{x_0}{\rho_s} \approx \frac{1}{2}\frac{1}{(\Omega_r+K)}\left(1 + i\frac{\Gamma(\Omega_r+2K)}{\Omega_r(\Omega_r+K)}\right)\left(\frac{L_n}{c_s}\right)\frac{\Omega_r^2}{s^2}\frac{d\bar{v}_{Ey}}{dx},$$

$$\Delta_k^2 \approx \left|\frac{\Omega_r\rho_s^2}{s}\right|\left(1 + i\frac{\Gamma}{\Omega_r}\right).$$

These coefficients combine to give a fluctuation intensity form factor with the structure,

$$|\Phi|^2 \sim A_\ell \exp\left\{-\left|\frac{s}{\Omega_r\rho_s^2}\right|\left|\frac{\Gamma}{\Omega_r}\right|\left[x - \left(x_{0r} - \frac{\Omega_r}{\Gamma}x_{0i}\right)\right]^2\right\}.$$

Hence the various terms in the effective shift of the profile form factor combine to take the simple form,

$$\frac{\xi}{\rho_s} = -\frac{1}{2}\frac{K}{(\Omega_r+K)^2}\left(\frac{L_n}{c_s}\right)\frac{\Omega_r^2}{s^2}\frac{d\bar{v}_{Ey}}{dx}.$$

b. Localization via Landau damping When $\zeta^{-1} \sim k_\parallel v_{ti}/\omega \sim O(1)$ the large parameter expansion of the Z function breaks down, and the effects of Landau damping start to become important. This defines a length scale related to the ion Landau resonance (i.e., Landau resonance points),

$$x_i \approx \pm\frac{L_s}{v_{ti}}\frac{\omega}{k_y}.$$

When these points are closer to the rational surface than the width of the spectrum as given in the previous section, the shape of the envelope is determined by the Landau damping.[36] In other words, if

$$\frac{\gamma}{\Omega_i} < \frac{\rho_i\rho_s}{L_sk_y^{-1}}$$

we can approximate the shape of the envelope as a step function, terminating at $x=x_i$. Of course within the step function, we will have the usual Pearlstein-Berk modes,[37] traveling outwards with a slow modulation due to the linear growth. The first obvious effect of the sheared flow on such a structure is simply to shift the central region (i.e., the region between the WKB turning points) within the step function. But this is completely irrelevant, as this shift does not directly modify the envelope structure, which is in fact determined by the Landau resonance points.

Physically, $\mathbf{E}\times\mathbf{B}$ flow shear also modifies the two Landau resonance points that are initially symmetric with respect to the rational surface by shifting both in the same direction (see Fig. 3). In other words,

$$x_i^{(+)} = \frac{\omega}{k_y}\frac{L_s}{(v_{\text{thi}} + L_sv'_{Ey})}, \quad x_i^{(-)} = -\frac{\omega}{k_y}\frac{L_s}{(v_{thi} - L_sv'_{Ey})}.$$

Hence the midpoint of the two shifts by an amount

$$\frac{\xi}{\rho_s} \approx -\frac{\Omega_r}{s^2}\frac{(L_n/c_s)v'_{Ey}(x)}{(\tau^{-1} - (L_n/c_s)^2v'_{Ey}(x)^2/s^2)} \approx -\tau\frac{\Omega_r}{s^2}\frac{L_n}{c_s}\frac{dv_{Ey}}{dx}.$$

We take this as the shift of the spectrum for this limit. Note that an $\mathbf{E}\times\mathbf{B}$ flow without shear would shift the Landau resonance points either towards or away from the origin and hence would not cause a *net* shift of the expectation value.

We have seen that the shift of the spectra, caused by the sheared $\mathbf{E}\times\mathbf{B}$ flow, has the generic form

$$\frac{\xi}{\rho_s} \approx -\alpha\frac{L_n}{c_s}\frac{dv_{Ey}}{dx},$$

where α is a dimensionless coefficient, previously introduced in Sec. II. Here α is positive for electron drift waves and negative for ITG, i.e.,

$$\alpha \approx \begin{cases} \tau\dfrac{\Omega_r}{s^2}, & \text{DW, } \dfrac{\gamma}{\Omega_i} < \dfrac{\rho_i\rho_s}{L_sk_y^{-1}} \\ \dfrac{K}{2s^2}\dfrac{\Omega_r^2}{(\Omega_r+K)^2}, & \text{DW, } \dfrac{\gamma}{\Omega_i} > \dfrac{\rho_i\rho_s}{L_ak_y^{-1}} \\ -\dfrac{K}{2}, & \text{ITG.} \end{cases}$$

V. MOMENTUM VERSUS FLOW

Up to this point, we have used a simple equation of motion for the parallel flow. Obviously (1) is not exact, as density gradient, magnetic curvature, and other effects on

this equation are neglected. A transport equation, governing the slow evolution of background toroidal momentum,[23] is more general,

$$\frac{\partial}{\partial t}\langle mnv_\phi\rangle + \nabla_r \Pi_\phi = m\Omega_i j_r + f_\phi. \tag{38}$$

Here $\langle mnv_\phi\rangle$ is the mean toroidal momentum, Π_ϕ is the flux of toroidal momentum, j_r is the radial current density, and f_ϕ is the toroidal component of the force density. Assuming $\langle mnv_\phi\rangle \approx m\langle n\rangle\langle v_\phi\rangle$, we can write

$$\Pi_\phi = m\langle nv_\phi v_{Er}\rangle = m(\langle n\rangle\Gamma_\phi + \langle v_\phi\rangle\Gamma_n). \tag{39}$$

Here $\Gamma_\phi \sim \langle v_{\mathrm{Er}} v_\phi\rangle \sim \langle v_{\mathrm{Er}} v_\parallel\rangle + (B_\theta/B_\phi)\langle v_{\mathrm{Er}} v_\chi\rangle$, where $\hat{\boldsymbol{\chi}} = \hat{\boldsymbol{b}} \times \hat{\boldsymbol{r}}$ is the binormal direction. We can solve (39) for Γ_ϕ since it is the toroidal flow, and not the momentum, which is actually measured.

However, it is the toroidal momentum that is the locally conserved field in the case when $f_\phi \approx j_r \approx 0$. Then in the spirit of turbulence equipartition theories,[38] the turbulent momentum flux can be written as a simple diffusion of toroidal momentum,

$$\Pi_\phi \sim -\chi_\phi m \nabla_r \langle nv_\phi\rangle. \tag{40}$$

Thus combining Eqs. (39) and (40), we can write

$$\Gamma_\phi \approx \frac{\Pi_\phi}{m\langle n\rangle} - \frac{\Gamma_n}{\langle n\rangle}\langle v_\phi\rangle \equiv -\chi_\phi \nabla_r \langle v_\phi\rangle + U_r\langle v_\phi\rangle,$$

where the last term is an effective inward momentum pinch driven by the outward particle flux, with a radial flow velocity, which is roughly

$$U_r \approx -\frac{\Gamma_n}{n} - \chi_\phi \frac{\nabla_r n}{n}. \tag{41}$$

It should be noted that for $\Gamma_n \sim -D_n\nabla_r n + V_r n$, if $\chi_\phi^{QL} \sim D_n^{QL}$, terms that are proportional to these coefficients would cancel each other and the turbulent radial flow would be proportional *only* to the neoclassical particle flux and the radial flow terms in the particle flux (i.e., the part that has the form $V_r\bar{n}$). We can write the equation for the toroidal flow as

$$\langle n\rangle \frac{\partial}{\partial t}\bar{v}_\phi + \nabla_r[\langle n\rangle\Gamma_\phi] = f_\phi.$$

Note that this depends on the assumption that the locally conserved field that is quasilinearly diffused is the angular momentum. The formulation of microturbulence drive on the flow based on (1)–(4) does not immediately lead to the form given in (40). Here we mention this formulation as a demonstration of the "recoil" effect of particle flux on toroidal flow. In other words, an ansatz based on momentum conservation (apart from quasilinear diffusion) leads to an effective torque proportional to the density gradient and the toroidal flow itself, and an effective flow (v_ϕ) pinch which is inward if the particle flux is outward and large. Physically, an outward particle flux leads to a drop in the toroidal momentum at a given radius (simply due to decrease of density), which must be compensated by an *increase* in toroidal speed if the toroidal momentum is to be conserved locally. Even though quasilinear diffusion causes local conservation (in the Eulerian sense) to break down, this pinch-like effect persists.

Note that the quasilinear microturbulence closure discussed in this paper does not give a substantial pinch for the parallel mean flow, which in turn motivated us to explore the effect of the particle pinch as the main pinch of toroidal momentum via the convective transport term. By way of contrast, in this paper we showed that if one uses toroidal momentum as the locally conserved, globally mixed field, the outward particle flux itself may appear as an inward pinch of toroidal flow. These two seemingly contradictory results highlight the fact that the main issue in understanding the transport of angular momentum is the identification of the locally conserved field (i.e., "canonical variables") and their relation to the physical observables. This, of course, depends on the types of microscopic processes that are responsible for the macroscopic fluxes (neoclassical versus anomalous, ITG versus electron drift waves, etc.), and the conservation laws for these microprocesses.

In order to numerically model the "recoil" effect discussed in this section we use a simplified version of our model with simple modifications in order to account for using a nonconserved field (i.e., $\bar{v}_\phi$). As usual, we set $F_\parallel = 0$. However, if we also set $\alpha = 0$ there is no spin up, and momentum can only be redistributed. In other words, $S(x)$ is necessary in order to get finite rotation without external drive. In any case, it is a common observation that diffusion of a conserved field usually leads to radial flow terms in the nonconserved field (i.e., terms explicitly proportional to the field itself). Thus, the $S(x)$ term and its physical basis remain roughly unmodified by a change of the dependent variable. The simplified model, which will be used for numerical computations, can be written as

$$\frac{\partial}{\partial t}\bar{v}_\phi + \frac{1}{\bar{n}}\frac{\partial}{\partial x}(\bar{n}\delta\Gamma_\phi) - \frac{1}{\bar{n}}\frac{\partial}{\partial x}\left[\bar{n}\alpha\varepsilon\left(1 - \sigma\frac{\partial}{\partial x}\bar{P}\right)\frac{\partial}{\partial x}\bar{v}_{Ey}\right] = 0, \tag{42}$$

$$\frac{\partial}{\partial t}\bar{n} + \frac{\partial}{\partial x}(\Gamma_n) = 0,$$

where

$$\Gamma_n = -[D_{\mathrm{neo}} + D_1\varepsilon]\frac{\partial\bar{n}}{\partial x} + U_r^{(n)}\varepsilon\bar{n}$$

and

$$\delta\Gamma_\phi = -(\nu_{\mathrm{neo}} + \nu_1\varepsilon)\nabla_r\langle v_\phi\rangle - \left(\frac{\Gamma_n}{\bar{n}} + \frac{\nu_1\varepsilon}{\bar{n}}\frac{\partial\bar{n}}{\partial x}\right)\langle v_\phi\rangle.$$

This simple model is completed with Eqs. (10), (12), and (14). Also, we set $\mu_2 = 0$ for simplicity. Note that if $\nu_1 \sim D_1$, the turbulent radial flow would be proportional to only the neoclassical particle flux and the particle pinch terms. The result of the numerical integration of this system for $U_r^{(n)} = 0.5$ can be seen in Fig. 9. Note that the parameters in this case are the same as the parameters in Fig. 5, even though the models are different. The results also seem somewhat similar. In fact, for this reason pressure and density profiles are not plotted. The flow, on the other hand, seems to have a

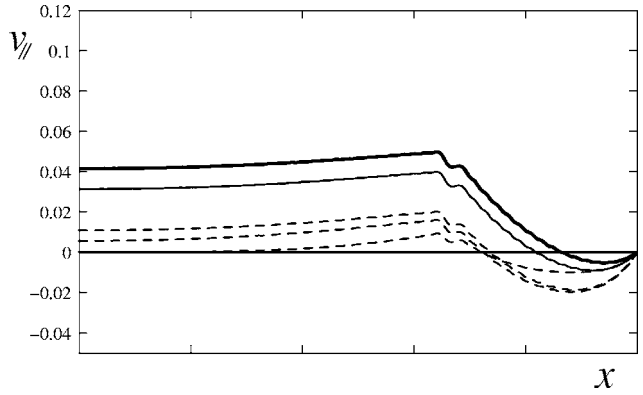

FIG. 9. Profile of parallel flow for the $F_{\|}=\mu_2=0$, $\mu_\beta=\beta=1.0$ case for Eq. (42). See Fig. 4 for a key.

surviving negative component near the edge region. Note that we did not perform parameter scans for this model since the difference was not enough to justify it. Also, even though the model seems to produce an "inward pinch" from outward particle flow, one should be careful, since the effect of the particle flow on the density profile is more drastic, which may lead to a relaxation of the edge gradients and this in turn reduces the more important effect of $S(x)$. We have also "tested" our numerical scheme in that if we set $S(x)=0$ and start with $\bar{v}_\phi(x)=0$ initially (also without external drive or boundary flow), we get $\bar{v}_\phi=0$ in all subsequent time steps. In short, even though the details of the profile changes between the models, the effect that ultimately rotates the plasma is the mean zero-flow component of the Reynolds stress, $S(x)$, in both cases.

VI. CONCLUSIONS

In this paper, we have presented a novel theory for the generation of intrinsic rotation at the $L\rightarrow H$ transition. The principal results of this paper are

1. The total flux of parallel momentum was calculated, and a convective inflow, associated with the particle pinch, was identified.
2. A general expression for the parallel Reynolds stress was derived and shown to have the form

$$\langle \tilde{v}_r \tilde{v}_\| \rangle \approx S(x) + V(x)\langle v_\| \rangle - \nu_T \frac{\partial \langle v_\| \rangle}{\partial x}.$$

   Explicit expressions for the flow-independent stress, $S(x)$, the convective flow $V(x)$, and turbulent viscosity $\nu_T(x)$ were derived. Note that $k_\| \rightarrow -k_\|$ is required for $S(x)\neq 0$ and $V(x)\neq 0$, and $S(x)$ has no analog in diffusion-convection models of the particle flux.
3. Sheared radial electric fields have been shown to break $k_\| \rightarrow -k_\|$ symmetry and render $S(x)$, $V(x)\neq 0$. In particular, nonzero $S(x)$ can drive net intrinsic rotation starting from a stationary plasma. Stationary rotation profiles are set by the competition between $S(x)$ and $\nu_T(x)$.
4. The momentum deposited in the plasma by the flow-independent stress $S(x)$ has its origins in the wave momentum of the fluctuations. Finite mean $\langle k_\| \rangle$ implies finite net wave momentum, which is ultimately absorbed at ion Landau resonance points and so transferred to the plasma. We show that these points are asymmetrically shifted in the same direction by the mean electric field shear, thus producing a net wave momentum and in turn a finite $S(x)$.
5. A self-consistent treatment of the electric field shear and the wave driven stress $S(x)$, the fluctuation intensity, and the turbulent viscosity ν_T reveals that the intrinsic rotation increases at the $L\rightarrow H$ transition, in accordance with the experimental observations. Intrinsic rotation results for $\langle v_\|(a)\rangle=0$, but will of course be stronger if edge momentum sources are present. Note that the effects of E_r' shear, and hence $S(x)$, were usually neglected in previous modeling attempts based on the dubious assumption that the effect of E_r' shear on toroidal rotation is small. We argue that, when all the dimensionless factors are taken into account, $S(x)$ can be as large as the diffusion term.
6. Since $S(x)$ is driven by the $(\nabla P/n)'$ piece of the electric field shear, the intrinsic rotation increases with plasma pressure, also in accordance with experimental observations.
7. The sensitivity of the intrinsic rotation to edge conditions has been examined.

Several caveats should be mentioned as well. First, this is only one of several possible mechanisms for understanding intrinsic rotation. Its strengths are its clear foundation in dynamics, and the fact that it clearly and directly links rotation to $L\rightarrow H$ transition, a trend which is clearly manifested in the phenomenology. Second, while a completely general theory is desirable, some degree of mode dependence is unavoidable, since the ratio $\omega_{E\times B}'/\omega_k$ appears frequently in the calculations. In particular, for ITG modes with $q'>0$, $S(x)$ is negative (i.e., inward) and $V(x)>0$ (outward), while for electron drift waves the opposite holds ($S>0$ and $V<0$). Third, in order to facilitate a consistent treatment of electric field shear effects, the theory presented here is cylindrical, and so we should add that additional toroidal effects may modify the momentum flux. In particular, toroidal effects can produce additional convection effects. Fourth, we cannot overemphasize the importance of boundary conditions and possible edge momentum sources in determining the intrinsic rotation. Further research on these is crucial to developing a predictive understanding of intrinsic rotation.

Finally, throughout this paper we have ignored the dynamics of poloidal rotation and assumed $\langle v_\theta \rangle$ to be well approximated by its small neoclassical value. However, in reality, poloidal and toroidal rotations are tightly coupled by the poloidal velocity contribution to $\langle E_r \rangle$, which enters via radial force balance (and this leads to cross diffusion via the effect of $\langle E_r \rangle'$ on toroidal momentum dynamics). Also, v_ϕ and v_θ are coupled due to the fact that $v_\| \approx v_\phi + v_\theta (B_\theta/B_\phi)$. This coupling can be accounted for by considering the self-consistent dynamics of the poloidal flow. Finally, toroidal and poloidal momenta are coupled by the radial current induced torque (N.B. $\langle J_r \rangle \sim \langle \tilde{v}_{Er} \nabla^2 \tilde{\Phi} \rangle \sim \partial \langle \tilde{v}_{Er} \tilde{v}_\theta \rangle / \partial r$, the poloidal Reynolds stress). Note also that radial current drives to-

roidal momentum via the $\mathbf{J}_r \times \mathbf{B}_\theta$ force and poloidal momentum via the $\mathbf{J}_r \times \mathbf{B}_\phi$ force. Since there are now experimental results which indicate a significant departure of $\langle v_\theta \rangle$ from the predicted neoclassical value, dual self-consistent treatments of both poloidal and toroidal rotations are ultimately required for a complete, definitive theory of momentum transport. Such a detailed analysis of the poloidal momentum transport is a large undertaking, well beyond the scope of this paper, and will be presented in a future work.

ACKNOWLEDGMENTS

We thank (in alphabetical order) C. S. Chang, J. deGrassie, X. Garbet, M. Greenwald, C. Hidalgo, K. Ida, A. Ince-Cushman, K. Itoh, S.-I. Itoh Y. Kamada, A. Peeters, J. Rice, W. Solomon, and M. Yoshida for stimulating discussions.

This research was supported by U.S. Department of Energy Grant No. FG02-04ER 54738 and Contract No. DE-AC02-76-CHO-3073, and the U.S. DOE SciDAC Center for Gyrokinetic Particle Simulation of Turbulent Transport in Burning Plasmas.

APPENDIX: CORRECTIONS TO REYNOLDS STRESS

We neglected higher-order corrections to the fluctuating parallel velocity (27) in the text. It is possible to continue the fluid expansion and include higher-order terms. The first few of those terms can be written as

$$\tilde{v}_\parallel^{(\text{higher order})} \approx -v_{ti}\frac{1}{\bar{\Omega}}\frac{e\tilde{\Phi}}{T_e}\left[b\left(\frac{\zeta^{-1}}{\sqrt{2}}(\pi\bar{\Omega}+1) - \frac{L_n}{v_{ti}}\frac{d\bar{v}_\parallel}{dx}\right) + \frac{\zeta^{-1}}{\sqrt{2}}\frac{x}{\rho_i}\frac{L_n}{v_{ti}}\frac{d\bar{v}_{Ey}}{dx}\right].$$

This also leads to a correction in the expression for the Reynolds stress, which can be written as

$$\langle \tilde{v}_{Ex}\tilde{v}_\parallel\rangle(\text{higher order}) = -\sum_k ic_s^2\left[\frac{k_\perp^2\rho_s^2}{\tau}\times\left(\left(\frac{c_s\rho_s k_y k_\parallel}{\omega}\right)\left(1+\frac{c_s\rho_s k_y}{L_n\omega}\tau^{-1}\right) - \frac{\rho_s^2 k_y^2}{\omega}\frac{d\bar{v}_\parallel}{dx}\right) + \left(\frac{c_s\rho_s k_\parallel k_y}{\omega}\right)\frac{c_s k_y}{\omega}\frac{x}{\rho_s}\frac{\rho_s}{c_s}\frac{d\bar{v}_{Ey}}{dx}\right]\left|\frac{e\tilde{\Phi}}{T_e}\right|^2.$$

Higher-order corrections for temperature are

$$\tilde{T}^{(\text{higher order})} = T_i\frac{e\tilde{\Phi}}{T_e}\frac{1}{\bar{\Omega}}\left[-b\eta_i - \frac{\sqrt{2}}{v_{ti}}\zeta^{-1}L_n\frac{d\bar{v}_\parallel}{dx} + (\pi\bar{\Omega}+1)\zeta^{-2} - \frac{\zeta^{-2}}{\sqrt{2}}\frac{x}{\rho_i}\frac{L_n}{v_{ti}}\frac{d\bar{v}_{Ey}}{dx}\right].$$

[1] S. D. Scott, P. H. Diamond, R. J. Fonck *et al.*, Phys. Rev. Lett. **64**, 531 (1990).
[2] N. Mattor and P. H. Diamond, Phys. Fluids **31**, 1180 (1988).
[3] K. Ida, Y. Miura, K. Itoh, S. Itoh, and T. Matsuda, J. Phys. Soc. Jpn. **67**, 4089 (1998).
[4] Y. Kusama, M. Yamamato, and JFT-2M Team, Fusion Sci. Technol. **49**, 89 (2006).
[5] I. H. Hutchinson, R. Boivin, F. Bombarda *et al.*, Phys. Plasmas **1**, 1511 (1994).
[6] J. E. Rice, W. D. Lee, E. S. Marmar *et al.*, Nucl. Fusion **44**, 379 (2004).
[7] B. LaBombard, J. E. Rice, A. E. Hubbard *et al.*, Phys. Plasmas **12**, 056111 (2005).
[8] J. R. Myra, J. Boedo, B. Coppi *et al.*, in *Proceedings of the 19th IAEA Fusion Energy Conference, Chengdu, China* (IAEA, Vienna, 2006), IAEA/TH-P6–21.
[9] M. Yoshida, Y. Koide, H. Takenaga *et al.*, in *Proceedings of the 19th IAEA Fusion Energy Conference, Chengdu, China* (IAEA, Vienna, 2006), IAEA/EX-P3–22.
[10] J. S. deGrassie, *Intrinsic Rotation in DIII-D*, APS-DPP Meeting, Philadelphia (2006).
[11] F. Hofmann, J. B. Lister, M. Anton *et al.*, Plasma Phys. Controlled Fusion **36**, B277 (1994).
[12] A. Bortolon, B. P. Duval, A. Pochelon, and A. Scarabosio, Phys. Rev. Lett. **97**, 235003 (2006).
[13] S. Ide and JT-60U Team, Phys. Plasmas **7**, 1927 (2000).
[14] M. Yoshida, Y. Koide, H. Takenaga *et al.*, Plasma Phys. Controlled Fusion **48**, 1673 (2006).
[15] B. Gonçalves, C. Hidalgo, M. A. Pedrosa, R. O. Orozco, E. Sanchez, and C. Silva, Phys. Rev. Lett. **96**, 145001 (2006).
[16] C. Hidalgo, B. Gonçalves, C. Silva, M. A. Pedrosa, K. Erents, M. Hron, and G. F. Matthews, Phys. Rev. Lett. **91**, 065001 (2003).
[17] J. E. Rice, A. Ince-Cushman, J. S. deGrassie *et al.*, "Inter-machine comparison of intrinsic toroidal rotation," Nucl. Fusion (to be published).
[18] *Technical Basis for the ITER Final Design*, ITER EDA Documentation Series Vol. 24 (IAEA, Vienna, 2001).
[19] P. H. Diamond, V. B. Lebedev, Y. M. Liang, A. V. Gruzinov, I. Gruzinova, and M. Medvedev, in *Proceedings of the 15th IAEA Fusion Energy Conference, Seville, Spain* (IAEA, Vienna, 1994), IAEA-CN-60/-2-II-6.
[20] X. Garbet, Y. Sarazin, P. Ghendrih, S. Benkadda, P. Beyer, C. Figarella, and I. Voitsekhovitch, Phys. Plasmas **9**, 3893 (2002).
[21] B. Coppi, Phys. Lett. A **201**, 66 (1995).
[22] B. Coppi, Nucl. Fusion **42**, 1 (2002).
[23] F. L. Hinton and S. K. Wong, Phys. Fluids **28**, 3082 (1985).
[24] H. Sugama and W. Horton, Phys. Plasmas **4**, 2215 (1997).
[25] K. C. Shaing, Phys. Plasmas **8**, 193 (2001).
[26] A. G. Peeters and C. Angioni, Phys. Plasmas **12**, 072515 (2005).
[27] A. K. Hansen, A. F. Almagri, D. Craig, D. J. D. Hartog, C. C. Hegna, S. C. Prager, and J. S. Sarff, Phys. Rev. Lett. **85**, 3408 (2000).
[28] B. A. Carreras, K. Sidikman, P. H. Diamond, P. W. Terry, and L. Garcia, Phys. Fluids B **4**, 3115 (1992).
[29] F. L. Hinton and G. M. Staebler, Phys. Fluids B **5**, 1281 (1993).
[30] R. R. Dominguez and G. M. Staebler, Phys. Fluids B **5**, 3876 (1993).
[31] F. Ebrahimi, V. V. Mirnov, S. C. Prager, and C. R. Sovinec, "Momentum transport from current-driven reconnection in the reversed field pinch," Phys. Rev. Lett. (to be published).
[32] T. Füllop, P. Helander, and P. J. Catto, Phys. Rev. Lett. **89**, 225003 (2002).
[33] S. Ku, C. S. Chang, M. Adams *et al.*, J. Phys.: Conf. Ser. **46**, 87 (2006).
[34] Ö. D. Gürcan, P. H. Diamond, and T. S. Hahm, Phys. Rev. Lett. **97**, 024502 (2006).
[35] M. Artun and W. M. Tang, Phys. Fluids B **4**, 1102 (1992).
[36] F. Y. Gang, P. H. Diamond, and M. N. Rosenbluth, Phys. Fluids B **3**, 68 (1991).
[37] L. D. Pearlstein and H. L. Berk, Phys. Rev. Lett. **23**, 220 (1969).
[38] M. B. Isichenko, A. V. Gruzinov, and P. H. Diamond, Phys. Rev. Lett. **74**, 4436 (1995).